CO-2271-20

# VACUUM STABILITY AND VACUUM EXCITATION IN A SPIN 0 FIELD THEORY

T. D. Lee and G. C. Wick

Columbia University
New York, N. Y. 10027



This research was supported in part by the U. S. Atomic Energy Commission.

## DISCLAIMER

## ABSTRACT

The theoretical possibility that in a limited domain in space, the expectation value $< \phi(x) >$ of a neutral spin 0 field may be abnormal (that is to say quite different from its normal vacuum expectation value) is investigated. It is shown that if the $\phi^3$-coupling is sufficiently large, then such a configuration can be metastable, and its physical size may become substantially greater than the usual microscopic dimension in particle physics. Furthermore, independent of the strength of the $\phi^3$-coupling, if $\phi(x)$ has a sufficiently strong scalar interaction with the nucleon field, the state that has an abnormal $< \phi(x) >$ inside a very heavy nucleus can become the minimum energy state, at least within the tree approximation; in such a state, the "effective" nucleon mass inside the nucleus may be much lower than the normal value. Both possibilities may lead to physical systems that have not yet been observed.

Contents


1. Introduction 1

2. Energy Density Function 11

3. Loop Diagrams

3.1 Prototype Diagrams 16

3.2 Renormalization 18

3.3 Loop Expansion 20

4. Stability

4.1 Non-degenerate Case 27

4.2 Degenerate Vacuum 31

5. Classical Solutions

5.1 One Spatial Dimension 33

5.2 Three-Dimensional Case 35

5.3 Constant External Source 37

5.4 External Source (Free Nucleon Gas) 44

5.5 External Source (Incompressible Nucleon Fluid) 53

6. $\sigma$ - Model 58

7. Remarks 65

Appendices 67

## 1. Introduction

In a relativistic field theory, the vacuum state is defined to be the lowest energy level of the system. In analogy with other quantum mechanical systems, however, a relativistic field may possess a degenerate lowest state. Perhaps the best known and simplest analogy is Heisenberg's infinite ferromagnet, in which case the degeneracy of the ground state is due to rotational invariance. The assumption of a degeneracy of the vacuum state, connected with a symmetry group of the Lagrangian, obviously has some far-reaching consequences, the most alluring of which is the possibility to "understand" that puzzling aspect of particle physics: the existence of broken symmetries. As is well-known, this has given rise to a host of interesting theoretical speculations.

Besides spontaneous symmetry breaking[1], and other well-known consequences[2] related to it (Goldstone bosons, Higgs phenomenon, etc.) the assumption of vacuum degeneracy, or near degeneracy, probably has other striking consequences, which have received little attention so far. We describe in the following an investigation of various questions, which arise naturally out of the virtual existence, within a given dynamical scheme, of states which could play the same role as the observed vacuum state, but are nevertheless different from it. We shall see that, depending on the details of the theory and on the values of certain physical parameters, which are not too well-known experimentally, there may or may not be consequences that are just as drastic as the already known features of this kind of theory.

All the schemes so far considered in the literature have two assumptions in common:

a) the Lagrangian of the system is invariant (or sometimes nearly invariant) under a certain group of transformations of the field variables;

b) in the (observed) lowest state of the system, some of the field variables have expectation values which are not invariant under all transformations of the symmetry group. Because of a) we must envisage the existence of other possible lowest states, or nearly lowest states, in which the expectation values of some of the fields are different; such states represent the abnormal vacuum states.

This is, of course, what is referred to in the literature as degeneracy of the vacuum; at the same time we are often reminded of the essential difference between this phenomenon, and the common variety of degenerate ground state encountered in finite systems: in the latter case all the states of a degenerate multiplet have the same degree of physical reality; the system can easily be induced to make transitions from one substate to the others. On the other hand, only one vacuum state is realized in our world; all the others are unphysical.

On second thoughts, the difference is not as profound as it seems. For the sake of clarity, and at the cost of repeating familiar things, let us recall in somewhat loose terms what is really implied. In a field theory of this type, the system possesses several "equivalent" configurations of minimum potential energy; in the observed lowest state the system performs small zero-point oscillations about one of these configurations. When the system is excited the configuration will deviate more strongly, but in any event only locally, from the basic equilibrium configuration. Fundamentally the stability of the situation is attributed to the infinite nature of the system; owing to this, the system will never flip over as a whole from the normally observed minimum

configuration, to one of the others, whose existence is required by the symmetry group. (As an example, the reader may recall what is usually said about the Heisenberg ferromagnet, spin waves, etc., and in particular the physical impossibility of rotating all the spins of an infinite ferromagnet simultaneously.)

Now in certain attempts at a sharp mathematical formulation of this state of affairs, it has even been asserted (perhaps on quite sound mathematical grounds) that in the limit of an infinite system one can construct a Hilbert space which contains only one "vacuum state", e.g. the observed one, and the excited states built upon it by local excitations. In this Hilbert space the physical quantities corresponding to local measurements are represented by well defined operators; some global quantities such as the total energy or momentum are also represented, we hope, but the global generators of the group are not.

It may seem, at first sight, that in this way one has neatly thrown the abnormal degenerate vacuum states out of the window, but physically it does not make so much difference, since in a certain sense they can reappear in the form of local excitations. In ferromagnetism the phenomenon is well-known under the name of domains of magnetization. More generally we argue as follows: suppose the configuration of the system flips over from the ordinary one to an abnormal equilibrium configuration, but only in a finite though large domain. As a volume effect, this will cost nothing; the difference in energy will be a relatively unimportant surface effect; in the case of a ferromagnet, for example, a very weak external field applied to a sufficiently large volume can easily cause the transition. Physical common sense suggests that any system with analogous features in the structure of the Lagrangian can exhibit similar phenomena under suitable

circumstances. The absolute stability of the asymmetric vacuum state is therefore a relative thing.

In this paper we intend to investigate the general question of vacuum stability, and in particular to inquire whether it is experimentally possible in a limited domain in space to "excite" (flip) the ordinary vacuum to an abnormal one. As we shall see, our discussion can be readily extended to include also theories that have no vacuum degeneracy, but only other local minima in the field energy. For definiteness, we shall first consider the simple theory of a renormalizable spin 0 Hermitian field $\phi$. The Lagrangian density is

$$\mathcal{L} = -\tfrac{1}{2}\left(\frac{\partial\phi}{\partial x_\mu}\right)^2 - U(\phi) + \text{counter terms} \qquad (1.1)$$

where

$$U(\phi) = \tfrac{1}{2} a \phi^2 + (3!)^{-1} b \phi^3 + (4!)^{-1} c \phi^4 \ , \qquad (1.2)$$

$\phi$ denotes the renormalized field operator, and $a$, $b$, $c$ are the appropriately defined renormalized constants. As usual, the counter-terms are for renormalization purposes; their precise definitions are given later in Section 3 and in Appendix A. In $U(\phi)$, the constant $c$ is assumed to be $> 0$ so that the energy spectrum has a lower bound. Through the transformation $\phi(x) \to \phi(x) +$ constant, one may always assume for the vacuum state

$$< \text{vac} \mid \phi(x) \mid \text{vac} > \ = \ 0 \ . \qquad (1.3)$$

Thus, $U(\phi)$ does not contain a linear term in $\phi$. [Note that in order to maintain

(1.3) there is a linear term in the counter terms. ] Furthermore, since the vacuum state is assumed to be the lowest energy state, the constant $a$ is also $>0$. For convenience, by using the transformation $\phi(x) \to -\phi(x)$, we may also choose the constant $b$ to be $\geq 0$. As a result, but without any loss of generality, the three constants $a$, $b$ and $c$ are all assumed to be positive.

To study the question whether there are other abnormal vacuum states, i.e., either degenerate or "excited" vacuum-like states, we find it convenient to first quantize the system in a box of a finite volume $\Omega$ with the periodic boundary condition, and then let $\Omega \to \infty$ in the end. A useful concept is to define an energy density function $\mathcal{E}(\bar{\phi})$:

$$\mathcal{E}(\bar{\phi}) \equiv \lim_{\Omega \to \infty} \Omega^{-1} \left[\text{minimum} < | H | >\right] \tag{1.4}$$

where $H$ is the total Hamiltonian and the minimum is taken among all states $|>$ under the constraint

$$\Omega^{-1} \int < | \phi(x) | > d^3r = \bar{\phi} \quad . \tag{1.5}$$

The value $\bar{\phi} = 0$ is, by definition, the minimum of $\mathcal{E}(\bar{\phi})$. Furthermore, it is convenient to adjust the constant part of the counter terms in (1.1) such that at the minimum $\bar{\phi} = 0$,

$$\mathcal{E}(0) = 0 \quad . \tag{1.6}$$

The problem whether there are other, either degenerate or "excited", vacuum-like

states then reduces simply to the investigation of the function $\mathcal{E}(\bar{\phi})$ for $\bar{\phi} \neq 0$, which turns out to have some rather interesting properties.

As will be shown in the next section, the dependence of $\mathcal{E}(\bar{\phi})$ on $\bar{\phi}$ bears a certain resemblance to the dependence of the Helmholtz free energy on the specific volume in thermodynamics. Just as in thermodynamics, when there is a phase transition, the Helmholtz free energy exhibits a straight-line dependence on the specific volume, its slope being the negative of the pressure; here, depending on the values of the renormalized constants a, b and c, the function $\mathcal{E}(\bar{\phi})$ may also contain a straight section, say between $\phi_\alpha \leqq \bar{\phi} \leqq \phi_\beta$. The existence of such a straight section appears to be a general feature of the theory, provided that the $\phi^3$-coupling constant b is sufficiently large. It exists even in the approximation of neglecting all loop diagrams; in such an approximation, one has $\mathcal{E}(\bar{\phi}) = U(\bar{\phi})$ <u>outside</u> the straight section, where U is given by (1.2). [Note that $U(\bar{\phi})$ does not contain any straight section.] Along the straight section $\phi_\alpha < \bar{\phi} < \phi_\beta$, the system actually comprises two phases, in analogy to the phase transition phenomenon in thermodynamics. Outside the straight section, $\bar{\phi} < \phi_\alpha$ or $\bar{\phi} > \phi_\beta$, the system exists only in a single phase. The "true" vacuum state $\bar{\phi} = 0$ is included in the region $\bar{\phi} > \phi_\beta$, as illustrated in Figure 1.

The inclusion of loop diagrams does not alter the general character of the energy density curve $\mathcal{E}(\bar{\phi})$. The explicit contributions of all one-loop and two-loop diagrams and some of the general properties of other multi-loop diagrams are given in Section 3. From these results, one expects that the function $\mathcal{E}(\bar{\phi})$ defined in either one of the two single-phase regions, say $\bar{\phi} < \phi_\alpha$, can be analytically continued beyond the point $\bar{\phi} = \phi_\alpha$ to the region $\bar{\phi} > \phi_\alpha$; its analytic continuation, called $\mathcal{E}_\alpha(\bar{\phi})$, is, of course,

different from $\mathcal{E}(\bar{\phi})$ in the two-phase region. [This phenomenon is again in close analogy to the familiar gas-liquid transition in statistical mechanics; the analytic continuation of the gas (or liquid) phase is the super-cooled gas (or super-heated liquid) region, not the two-phase region[3]. ] Similarly, one may analytically continue the function $\mathcal{E}(\bar{\phi})$, defined in the other single-phase region $\bar{\phi} > \phi_\beta$, to the region $\bar{\phi} \leqq \phi_\beta$ and call its analytic continuation $\mathcal{E}_\beta(\bar{\phi})$. In general, one expects the function $\mathcal{E}_\alpha(\bar{\phi})$ to have a minimum at

$$\bar{\phi} = \phi_{vex} \tag{1.7}$$

where the subscript "vex" denotes the vacuum excitation state.

In the case of the degenerate vacuum, both the true vacuum state $\bar{\phi} = 0$ and the vacuum excitation state $\bar{\phi} = \phi_{vex}$ appear as the endpoints of the straight section $\phi_\alpha \leqq \bar{\phi} \leqq \phi_\beta$; i.e.,

$$\phi_\alpha = \phi_{vex} \quad , \qquad \phi_\beta = 0$$

and because of (1.6)

$$\mathcal{E}(\phi_\alpha) = \mathcal{E}(\phi_\beta) = 0 \ . \tag{1.8}$$

From (1.2), one sees that if all loop diagrams are neglected, then the degeneracy occurs at

$$3ac = b^2 \ . \tag{1.9}$$

As we shall discuss in Section 3, there is a simple and convenient way to define the renormalization constants, so that (1.9) is the exact condition for degeneracy when all the loop diagrams are also included. Consequently, in order that the absolute minimum energy level is at $\bar{\phi} = 0$, we must have

$$3ac \geqq b^2 \ ; \tag{1.10}$$

otherwise, the role of the states $\bar{\phi} = 0$ and $\bar{\phi} = \phi_{vex}$ will be interchanged.

In Section 4, we study the question of the lifetime of the system in the excited state $\bar{\phi} = \phi_{vex}$. We shall show that in the non-degenerate case $(3ac > b^2)$, as the volume $\Omega \to \infty$, the lifetime becomes zero. On the other hand, there may exist metastable states which satisfy approximately

$$< | \phi(x) | > \ = \ \phi_{vex} \tag{1.11}$$

in a finite volume $L^3$, where $L$ is $\gg m^{-1}$ and $m^{-1}$ denotes the relevant microscopic length in the problem; $m$ can be either $\sim O(b)$, or $O(a^{\frac{1}{2}})$. Outside the volume, except over a surface region of a volume $\sim O(L^2 m^{-1})$, one has $< | \phi(x) | > = 0$. The excitation energy of such a state in its rest frame is given by

$$M_{vex} \ = \ L^3 \mathcal{E}_\alpha(\phi_{vex}) + O(L^2 m^3) \tag{1.12}$$

where $O(L^2 m^3)$ denotes the surface energy and $\mathcal{E}_\alpha(\bar{\phi})$ is the aforementioned analytic continuation of $\mathcal{E}(\bar{\phi})$. The lifetime $\tau$ of such a state is given by

$$\tau \gtrsim L \ , \qquad (1.13)$$

provided $\ln(Lm)$ is not too large, though $(Lm)$ must be $\gg 1$. Only in the special case of a vacuum degeneracy; i.e., $\mathcal{E}_a(\phi_{vex}) = 0$, can the size $L$ be arbitrarily large; its rest mass is determined completely by the surface energy. In general, the ratio of the width to the rest mass of such vacuum excitations in either the degenerate or the non-degenerate case is exceedingly small, given by

$$(\tau M_{vex})^{-1} \lesssim \left[L^4 \mathcal{E}_a(\phi_{vex}) + O(L^3 m^3)\right]^{-1} \ll 1 \ . \qquad (1.14)$$

In Section 5, we discuss the classical solutions corresponding to the vacuum excitations. The most interesting aspect of these solutions occurs when there is an extended external source. For definiteness, we may treat approximately the effect of a heavy nucleus as that of an "external source", assuming that there is a strong interaction $g\psi^\dagger\gamma_4\psi\phi$ between the scalar field $\phi$ and the nucleon field $\psi$. As we shall see, within the tree approximation, if the surface energy can be neglected, then when $g$ is sufficiently strong, or when the nuclear density is sufficiently high, the lowest energy state becomes one in which the expectation value $<\phi(x)>$ inside the nucleus can be quite different from its normal vacuum expectation value (which is zero, by our convention). Furthermore, inside the nucleus the "effective" mass of the nucleon becomes $m_N + g<\phi>$, which can also be quite different from its normal value $m_N$.

A concrete example of such a strong interaction is given by the well-known $\sigma$-model. This is examined in Section 6. It appears that, within the tree approximation, if the mass of the $\sigma$-particle is $\lesssim$ a few GeV, there may well exist a new family of metastable, or even stable, super-heavy nuclei.

By taking the zero pion mass limit, our discussion of the $\sigma$-model can be readily extended to theories with Goldstone bosons; with some further minor modifications, it can also be applied to fields with Higgs mechanisms.

## 2. Energy Density Function

To evaluate the energy density function $\mathcal{E}(\bar{\phi})$, defined by (1.4), we apply the standard Lagrangian multiplier method to take into account the constraint (1.5). Let $H_J$ be a new Hamiltonian, defined by

$$H_J \equiv H + J \int \phi(x)\, d^3r \tag{2.1}$$

where $J$ is the Lagrangian multiplier, and $H$ is the original Hamiltonian, which according to (1.1) is given by

$$H = \int \left[ \tfrac{1}{2} \Pi^2 + \tfrac{1}{2} (\nabla\phi)^2 + U(\phi) + \text{counter terms} \right] d^3r \tag{2.2}$$

and $\Pi$ is the conjugate momentum of $\phi$. Let the lowest eigenvalue of $H_J$ be $\Omega\lambda_J$; i.e.,

$$H_J \,|> \;=\; \Omega\lambda_J \,|> \;. \tag{2.3}$$

By using (2.1), (1.4) and (1.5), we find the energy density function $\mathcal{E}(\bar{\phi})$ to be given by the Legendre transformation

$$\mathcal{E}(\bar{\phi}) = \lambda_J - J\bar{\phi} \tag{2.4}$$

where

$$\bar{\phi} = \frac{\partial \lambda_J}{\partial J} \tag{2.5}$$

and

$$J = - \frac{\partial \mathcal{E}(\bar{\phi})}{\partial \bar{\phi}} \quad . \tag{2.6}$$

To calculate $\lambda_J$, let us decompose

$$H_J = H_0 + H_1 \tag{2.7}$$

where

$$H_0 = \tfrac{1}{2} \int \left[ \pi^2 + (\nabla\phi)^2 + \tfrac{1}{2} a \phi^2 \right] d^3r \quad , \tag{2.8}$$

and regard $H_1$ as a perturbation. The power series expansion of $\lambda_J$ in terms of the constants $J$, $b$ and $c$ can be readily derived. Following the treatment given by S. Coleman and E. Weinberg[4] (which is also formally analogous to some of the analysis developed in statistical mechanics and many-body problems[5]), we may regroup the perturbation series expansion of $\lambda_J$ into sums of tree diagrams, one-loop diagrams, two-loop diagrams, etc. The systematics of these loop diagrams will be given in the next section. Here, we only discuss the tree approximation. It is not difficult to see[6] that in the tree approximation $\lambda_J$ is given by the absolute minimum of

$$U_J(\phi) \equiv J\phi + U(\phi) = J\phi + \tfrac{1}{2} a\phi^2 + (3!)^{-1} b\phi^3 + (4!)^{-1} c\phi^4 \quad , \tag{2.9}$$

and $\phi = \bar{\phi}$ is the minimum point. [For completeness, a proof is given in Appendix A.] At $J = 0$, one has $U_J = U$. Since we are interested in the case where the function $U(\phi)$ in the original Lagrangian (1.1) has more than one local minimum, the $\phi^3$-coupling constant $b$ cannot be too small:

$$b^2 > \frac{8}{3} a c \quad . \tag{2.10}$$

On the other hand, because of our convention that the absolute minimum of $U(\phi)$ should be at $\phi = 0$, we have

$$b^2 \leq 3ac \quad . \tag{2.11}$$

[The apparent narrow region defined by these two inequalities may be deceptive. Actually, only (2.10) is the relevant one. If $b^2$ is $> 3ac$, then the absolute minimum of $U$ is not at $\phi = 0$. By using the transformation $\phi \to \phi +$ constant, this absolute minimum can be shifted back to $\phi = 0$. Under such a transformation, only the coupling constant $c$ is invariant; the new constants $a$ and $b$ now satisfy $b^2 < 3ac$.]

Next, we consider the equation $\frac{\partial U_J}{\partial \phi} = 0$; i.e., on account of (2.9),

$$J = -\frac{\partial U}{\partial \phi} = -a\phi - \tfrac{1}{2}b\phi^2 - (3!)^{-1}c\phi^3 \tag{2.12}$$

which at $J = 0$ has three roots:

$$\phi = 0 \quad \text{and} \quad \phi = \phi_{\pm} \equiv \frac{3}{2c}\left[-b \pm (b^2 - \frac{8}{3}ac)^{\frac{1}{2}}\right] . \tag{2.13}$$

Among these, $\phi = 0$ is the absolute minimum of $U(\phi)$, $\phi = \phi_+$ is a local maximum and $\phi = \phi_-$ is the other local minimum. As $J$ increases, these two minima will move, and the corresponding values of $U(\phi)$ will also change. There is a critical value $J_c$ at which these two minima become degenerate. As illustrated in Figure 1, we may determine graphically the value $J = J_c$ by using Maxwell's rule of equal area. The absolute minimum $\phi = \bar{\phi}$ makes a sudden jump from $\bar{\phi} = \phi_\beta$ at $J = J_{c-}$ to $\bar{\phi} = \phi_\alpha$ at $J = J_{c+}$.

By using (2.4) we find in the tree approximation

$$\mathcal{E}(\bar{\phi}) = U(\bar{\phi})$$

in the region

$$\bar{\phi} \geqq \phi_\beta \qquad \text{and} \qquad \bar{\phi} \leqq \phi_\alpha \quad . \tag{2.14}$$

But in $\phi_\alpha \leqq \bar{\phi} \leqq \phi_\beta$, $\mathcal{E}(\bar{\phi})$ is a linear function of $\bar{\phi}$, which is simply the common tangent line of $U(\bar{\phi})$ at $\bar{\phi} = \phi_\alpha$ and $\phi_\beta$.

Such behavior is analogous to the problem of phase transition in statistical mechanics. In the statistical analog, the roles of $J$, $\bar{\phi}$, $\mathcal{E}(\bar{\phi})$ and $\lambda_J$ are replaced by those of pressure, specific volume, Helmholtz free energy density and Gibbs free energy density, respectively. The straight section $\phi_\alpha \leqq \bar{\phi} \leqq \phi_\beta$ denotes the two-phase region. As already noted in the introduction, the function $\mathcal{E}(\bar{\phi})$ in either one of the single-phase regions, $\bar{\phi} > \phi_\beta$ or $\bar{\phi} < \phi_\alpha$, can be analytically continued into the two-phase region. In the tree approximation, these two analytic continuations are identical and both lead to $U(\bar{\phi})$. This is again analogous to the Van der Waals approximation used in statistical mechanics. In statistical mechanics, the analytic continuations of the thermodynamical functions of the liquid and the gas phases are respectively those of the super-heated liquid and the super-cooled gas, which should be different functions, but they reduce to the same expression in the Van der Waals approximation.

In the present problem, except for the degenerate vacuum case, the energy density function $\mathcal{E}(\bar{\phi})$ has only one minimum at $\bar{\phi} = 0$, and that is the true vacuum state. On the other hand, if the $\phi^3$-coupling constant $b$ is not too small, the

analytic continuation of $\mathcal{E}(\bar{\phi})$ is expected to have another minimum at $\bar{\phi} = \phi_{vex}$ which denotes the vacuum excitation. In the above, this property has been established in the tree approximation; as we shall see in the next section, if the coupling c is not too large, this property remains correct at least to every order in the loop expansion.

## 3. Loop Diagrams

The reduction of the perturbation series expansion of $\mathcal{E}(\bar{\phi})$ into a sum of tree diagrams, one-loop diagrams, etc. has been given in Ref. 4. In this section, we shall first briefly review the procedure, and then discuss some new properties.

### 3.1 Prototype Diagrams

By using the free field Hamiltonian $H_0$, defined by (2.8), as the unperturbed Hamiltonian, one can readily expand the energy density function $\mathcal{E}(\bar{\phi})$ as a power series in $b$, $c$ and $\bar{\phi}$. As will be shown in Appendix A, we may separate $\mathcal{E}(\bar{\phi})$ into a sum of tree diagrams and loop diagrams:

$$\mathcal{E}(\bar{\phi}) = \left[\mathcal{E}(\bar{\phi})\right]_{\text{tree}} + \sum_{\ell=1}^{\infty} \left[\mathcal{E}(\bar{\phi})\right]_{\ell\text{-loop}} \tag{3.1}$$

where $\left[\mathcal{E}(\bar{\phi})\right]_{\ell\text{-loop}}$ represents the summation over all one-particle irreducible scattering diagrams that have $\ell$ loops and in which every external line carries a zero 4-momentum and contributes a factor $\bar{\phi}$ to the Feynman integral. For the tree diagrams (away from the two-phase region), one has

$$\left[\mathcal{E}(\bar{\phi})\right]_{\text{tree}} = U(\bar{\phi}) \tag{3.2}$$

where $U$ is given by (1.2), provided that the renormalized constants $a$, $b$ and $c$ in $U(\bar{\phi})$ are related to the appropriate scattering amplitudes at zero momentum. [See Section 3.2 and Appendix A for further discussions of renormalization.]

For $\ell \neq 0$, it is useful to introduce $D(k)$, defined to be the propagator of the spin 0 particle moving in a given constant external field $\phi_{ext}$ whose value happens to be given by $\phi_{ext} = \bar{\phi}$. Thus, $D(k)$ is identical to the propagator of a free particle, but with its $(\text{mass})^2$ given by $(\partial^2 U/\partial\bar{\phi}^2)$; i.e.,

$$D(k) = -i\left[k^2 + a(1+\Delta)\right]^{-1} \tag{3.3}$$

where

$$\Delta = \bar{\phi}(b + \tfrac{1}{2}c\bar{\phi})/a \quad . \tag{3.4}$$

Let us first consider the sum of all one-loop diagrams, and differentiate $\left[\mathcal{E}(\bar{\phi})\right]_{\text{one-loop}}$ with respect to $a$, but keeping $b$, $c$ and $\bar{\phi}$ fixed. We obtain

$$\frac{\partial}{\partial a}\left[\mathcal{E}(\bar{\phi})\right]_{\text{one-loop}} = \int (2\pi)^{-4}\, d^4k \left[D(k) + \text{subtraction term}\right] \tag{3.5}$$

which can be readily established by first expanding both sides as a power series of $\bar{\phi}$, then noting that graphically the differentiation $\frac{\partial}{\partial a}$ on the one-loop diagram is just like cutting open one of its internal lines; this turns each loop diagram into a propagator diagram. Thus, diagram by diagram, both sides of (3.5) are equal. The subtraction term in (3.5) is needed to eliminate divergences. [The details of the subtraction term will be given below in Section 3.2.] From Eq. (3.5), it follows that[4,5]

$$\left[\mathcal{E}(\bar{\phi})\right]_{\text{one-loop}} = i\int (2\pi)^{-4}\, d^4k \left(\ln\left[i\,D(k)\right] + \text{subtraction term}\right). \tag{3.6}$$

Throughout the paper, $k^2 = \vec{k}^2 - k_0^2$ and $d^4k$ is real.

It is straightforward to express the higher order loop diagrams in terms of $D(k)$. In this way all external lines attached to a three-point vertex and all pairs of external lines attached to a four-point vertex are implicitly accounted for. We need only consider those $\ell$-loop diagrams, called prototype diagrams[4,7], in which all external lines, if they exist, must be attached separately to different four-point vertices; i.e., every three-point vertex $b\phi^3$ connects only internal lines and every four-point vertex $c\phi^4$ connects at most one external line to the diagram. For any given $\ell > 1$, there are only a finite number of such prototype diagrams. We shall evaluate these prototype diagrams according to the standard Feynman rule, except that each internal line gives a factor $D(k)$, not $-i(k^2+a)^{-1}$, to the Feynman integral. Otherwise, all the remaining factors in the Feynman integral are as usual; i.e., we assign factors $b$, $c$ and $\bar{\phi}$ respectively for a three-point vertex, a four-point vertex and an external line. Except for the subtraction terms that are needed for renormalization purposes (and which will be discussed below in Section 3.2), the function $\left[\mathcal{E}(\bar{\phi})\right]_{\ell\text{-loop}}$ for $\ell > 1$ is simply given by the sum over the finite set of all different prototype $\ell$-loop diagrams. As an example, for $\ell = 2$, there are only four different prototype diagrams; these are given by diagrams (i) - (iv) in Figure 2. [Because of renormalization, one must combine these four diagrams together with diagrams (ii)', (iii)' and (iv)' in Figure 2. The explicit value of these two-loop diagrams is given in Section 3.3.]

## 3.2 Renormalization

In (3.6), the integral $\int d^4k \ln(iD)$ is quartically divergent, therefore three subtractions are needed to eliminate the infinities. The corresponding subtraction term

should be at least a quadratic function in $\bar{\phi}$. However, it is entirely a matter of choice whether or not one should also subtract the finite $\bar{\phi}^3$ and $\bar{\phi}^4$ terms from the integral. Similar ambiguities also exist for higher order loop diagrams. This problem is closely tied to the original freedom in defining the renormalized constants a, b and c. Any finite loop-diagram contribution to the $\bar{\phi}^3$ and $\bar{\phi}^4$ terms can either be included in the renormalized constants [i.e., already included in the $b\bar{\phi}^3$ and $c\bar{\phi}^4$ terms in the original $U(\bar{\phi})$ function given by (1.2)], or otherwise. If they are included, then a corresponding subtraction is necessary in the relevant loop calculation to avoid double counting, but otherwise not. As it turns out, there is a particularly convenient way to decide on which choice to make.

Let us first consider the special case of degenerate vacuum. If $3ac = b^2$, the function $U(\phi)$ in the original Lagrangian (1.1) is symmetric with respect to the transformation

$$\phi + \frac{b}{c} \rightarrow -(\phi + \frac{b}{c}) \quad . \tag{3.7}$$

It is clearly desirable that the symmetry should also be maintained by the counter terms; in that case the entire Lagrangian (1.1) is invariant under the same transformation, and consequently the vacuum degeneracy becomes an exact property. It is quite simple to show that the dependence of $[\mathcal{E}(\bar{\phi})]_{\ell\text{-loop}}$ on $\bar{\phi}$, except maybe for the subtraction terms, is completely through the variable $\Delta$, given by (3.4). Since $\Delta$ is invariant under the transformation $(\bar{\phi} + \frac{b}{c}) \rightarrow -(\bar{\phi} + \frac{b}{c})$, the same symmetry holds for $\mathcal{E}(\bar{\phi})$ if all these subtraction terms in the loop-diagram calculations are also functions of $\Delta$. Because $\Delta$ is a quadratic function of $\bar{\phi}$ and because these subtraction terms should be at most quartic functions of $\bar{\phi}$, we require them to be quadratic functions of $\Delta$.

Thus, in a power series expansion in $\Delta$

$$\left[ \mathcal{L}(\bar{\phi}) \right]_{\ell\text{-loop}} = \alpha \Delta^3 + \beta \Delta^4 + \gamma \Delta^4 + \cdots \tag{3.8}$$

where $\alpha$, $\beta$, $\gamma$, $\cdots$ are constants. As a result, if $3ac = b^2$, the entire Lagrangian is symmetric under (3.7), and that implies a degenerate vacuum. In the following, the requirement (3.8) will be imposed also for the general case, even when there is no degeneracy.

With this requirement, and the convention that $\bar{\phi} = 0$ denotes the true vacuum, we derive the inequality

$$b^2 \leqq 3ac \ , \tag{3.9}$$

which is the same as (2.11), but is now valid with the inclusion of all loop-diagram corrections, not just in the tree approximation.

### 3.3 Loop Expansion

In order to understand the nature of the loop expansion, we establish first the following theorem:

Theorem 1. At any $\ell \geqq 1$, $\left[ \mathcal{L}(\bar{\phi}) \right]_{\ell\text{-loop}}$ can be written in terms of $\ell$ dimensionless functions $F_{\ell,1}$, $F_{\ell,2}$, $\cdots$, $F_{\ell,\ell}$ which depend only on $\Delta$ :

$$\left[ \mathcal{L}(\bar{\phi}) \right]_{\ell\text{-loop}} = a^2 \sum_{m=1}^{\ell} c^{m-1} \left[ a^{-1}(b^2 + 2ac\,\Delta) \right]^{\ell - m} F_{\ell,m}(\Delta) \tag{3.10}$$

where $\Delta$ is given by (3.4).

Proof. Let us consider an $\ell$-loop prototype diagram with $N$ three-point vertices, $M$ four-point vertices, $E$ external lines and $I$ internal lines. From the explicit Feynman rules given above, it follows that the corresponding Feynman integral for $\mathcal{E}(\bar{\phi})$ is of the form

$$b^N c^M \bar{\phi}^E f(a, \Delta) \quad . \tag{3.11}$$

Since the total number of loops is given by $\ell = I - N - M + 1$ and since $(2I + E)$ is equal to $(3N + 4M)$, we have

$$\ell = \tfrac{1}{2} N + M - \tfrac{1}{2} E + 1 \quad . \tag{3.12}$$

The a-dependence in (3.11) can be easily obtained from a simple dimensional analysis. Because $\Delta$ and $c$ are both dimensionless, but $a$, $b^2$, $\bar{\phi}^2$ and $\left[\mathcal{E}(\bar{\phi})\right]^{\frac{1}{2}}$ are of the same dimension $(\text{mass})^2$, we obtain

$$f(a, \Delta) = a^{2 - \frac{1}{2}(N+E)} F(\Delta) \tag{3.13}$$

where $F$ is dimensionless. For the special case of $E = 0$ [i.e., those prototype diagrams with no external line $\bar{\phi}$], by using (3.11)-(3.13), we find that the Feynman integral of such a diagram is of the form

$$a^2 c^M (b^2/a)^{\ell - M - 1} F(\Delta) \quad . \tag{3.14}$$

Now, from the definition of prototype diagrams we see that any $E \neq 0$ prototype

diagram can be transformed into an $E = 0$ prototype diagram by simply replacing all four-point vertices that are attached to external lines by three-point vertices, but keeping all internal lines and other vertices unchanged. Formally, we may represent such a replacement by

$$c\bar{\phi}\phi_{in}^3 \rightarrow b\phi_{in}^3 \tag{3.15}$$

where $\phi_{in}$ denotes the appropriate internal line and $\bar{\phi}$ the external line. Thus, the sum over all different prototype diagrams that can be transformed into the same $E \neq 0$ prototype diagram through (3.15) is equal to the Feynman integral of the $E = 0$ diagram, provided we change $b \rightarrow (b + c\bar{\phi})$; therefore, (3.14) becomes

$$a^2 c^M \left[a^{-1}(b^2 + 2ac\Delta)\right]^{\ell - M - 1} F(\Delta) \quad .$$

Since $M$ can vary from $0$ to $\ell - 1$, Theorem 1 is proved.

Remarks. According to (3.9), $b^2$ is $\leq 3ac$; we may regard the loop expansion as a power series expansion in $c$, but treating $\Delta$ and $(b^2/ac)$ [and therefore also $(b\bar{\phi}/a)$ and $(c\bar{\phi}^2/a)$] as $\lesssim 0(1)$.

Theorem 2.

$$\left[\mathcal{E}(\bar{\phi})\right]_{\text{one-loop}} = \frac{a^2}{32\pi^2}\left[\tfrac{1}{2}(1+\Delta)^2 \ln(1+\Delta) - \frac{\Delta}{2} - \tfrac{3}{4}\Delta^2\right] \tag{3.16}$$

and

$$\left[\mathcal{E}(\bar{\phi})\right]_{\text{two-loop}} = \frac{2a^2c}{(32\pi^2)^2}\left[(1+\Delta)\ \ln(1+\Delta) - \Delta\right]^2$$

$$+ \frac{2a(b^2+2ac\Delta)}{(32\pi^2)^2}\left\{\tfrac{1}{2}(1+\Delta)\left[\ln(1+\Delta)\right]^2 - 2(1+\Delta)\ln(1+\Delta) + 2\Delta + \tfrac{1}{2}\Delta^2\right\}. \tag{3.17}$$

Proof. The evaluation of $\left[\mathcal{E}(\bar{\phi})\right]_{\text{one-loop}}$ follows readily from (3.6) and (3.8); the result is (3.16). [If $b = 0$, that is in the pure $\phi^4$ theory, the above expression for $\left[\mathcal{E}(\bar{\phi})\right]_{\text{one-loop}}$ reduces to the form derived by Coleman and Weinberg[4]. ] The two-loop prototype diagrams are listed in Figure 2. These diagrams can be calculated according to the general rules given in the previous sections. The calculation is somewhat involved because of renormalization. The details are given in Appendix B, and the result is (3.17).

The evaluation of higher order loop diagrams is complicated partly because of the large number of diagrams and partly because of the renormalization procedures required to eliminate infinities. For simplicity, we shall consider the special case $c = 0$. In such a case, there are only the $b\phi^3$ vertices, and the theory is super-renormalizable. The Feynman integrals of the majority of the $\ell$-loop diagrams are convergent. In the following theorem, we shall restrict our discussion to these convergent diagrams, or "primitively divergent" diagrams as in the case of $\ell = 3$. [A "primitively divergent" diagram, as defined by Dyson[8], is one whose Feynman integral, though divergent, becomes convergent when any one of its internal momenta is held fixed; here, the only example is in $\ell = 3$. ]

Theorem 3 (proved in Appendix C). If $c = 0$ and if we include only convergent, or "primitively divergent", diagrams, then

$$\left[\mathcal{E}(\bar{\phi})\right]_{\text{three-loop}} = (\text{constant})\, b^4 \left[\ln(1+\Delta) - \Delta + \tfrac{1}{2}\Delta^2\right] \qquad (3.18)$$

and for $\ell > 3$

$$\left[\mathcal{E}(\bar{\phi})\right]_{\ell\text{-loop}} = (\text{constant})\, a^2 (b^2/a)^{\ell-1} \left[(1+\Delta)^{3-\ell} - 1 + (\ell-3)\Delta - \tfrac{1}{2}(\ell-3)(\ell-2)\Delta^2\right] . \qquad (3.19)$$

Remarks. From Theorem 2 and Theorem 3, it follows that every term in the loop expansion is singular at $\Delta = -1$; i.e.,

$$\bar{\phi} = c^{-1}\left[-b \pm (b^2 - 2ac)^{\frac{1}{2}}\right] , \qquad (3.20)$$

which are the points of inflexion A and B of the function $U(\bar{\phi})$, as illustrated in Figure 1. This implies that the energy density function $\mathcal{E}(\bar{\phi})$ can be analytically continued from either one of the two single-phase regions, $\bar{\phi} < \phi_\alpha$ or $\bar{\phi} > \phi_\beta$, to the two-phase region. Let $\mathcal{E}_\alpha(\bar{\phi})$ denote the analytic continuation from $\bar{\phi} < \phi_\alpha$, and $\mathcal{E}_\beta(\bar{\phi})$ that from $\bar{\phi} > \phi_\beta$. If the loop expansion is used, then $\mathcal{E}_\alpha(\bar{\phi})$ has a singularity at A, and $\mathcal{E}_\beta(\bar{\phi})$ a singularity at B. [At $\Delta = -1$, the propagator $D(k)$ is that of a zero-mass particle. Thus, physically, it seems reasonable that there should be such singularities for these analytic continuations, independent of the loop expansion.] The true vacuum is at $\bar{\phi} = 0$, and therefore it lies in the single phase region $\bar{\phi} > \phi_\beta$.

The vacuum excitation $\bar{\phi} = \phi_{vex}$ denotes the minimum of the analytic continuation $\mathcal{E}_a(\bar{\phi})$. From Figure 1, one sees that the point $\bar{\phi} = \phi_{vex}$ lies in between $\phi = \phi_a$ and the $\bar{\phi}$ corresponding to A.

In Figure 3, we plot the modification of the J vs. $\bar{\phi}$ curve due to the one-loop diagram for the special case $b^2 = 3ac$. Because of the symmetry under the transformation (3.7), the two-phase region, with the inclusion of the loop-diagram correction, remains given by

$$J = 0 \qquad \text{and} \qquad -\frac{2b}{c} \leqq \bar{\phi} \leqq 0 \ . \tag{3.21}$$

It is convenient to introduce the dimensionless variables $X$, $V$ and $j$, defined by

$$\bar{\phi} \equiv \frac{b}{c}(X-1) \ , \qquad \mathcal{E} \equiv \frac{ab^2}{c^2} V$$
$$J \equiv \frac{ab}{c} j \ , \tag{3.22}$$

and therefore $j = -\dfrac{\partial V}{\partial X}$. From (3.2) and (3.16), we have (for the special case $b^2 = 3ac$)

$$V_{tree} = \tfrac{1}{8}(1-X^2)^2 \tag{3.23}$$

and

$$V_{one\text{-}loop} = \tfrac{1}{3}\gamma\left[\tfrac{1}{2}(1+\Delta)^2 \ln(1+\Delta) - \frac{\Delta}{2} - \tfrac{3}{4}\Delta^2\right] \tag{3.24}$$

where

$$\Delta = \tfrac{3}{2}(X^2-1) \tag{3.25}$$

and

$$\gamma = \frac{c}{32\pi^2} \quad . \tag{3.26}$$

In Figure 3, for definiteness we assume arbitrarily

$$\gamma = 10^{-1} \quad . \tag{3.27}$$

## 4. Stability

In this section we discuss the stability problem if the system is not in the true vacuum state $\bar{\phi} = 0$, but in the vacuum excitation state $\bar{\phi} = \phi_{vex}$. As remarked before, only in the case of a degenerate vacuum do both $\bar{\phi} = 0$ and $\bar{\phi} = \phi_{vex}$ lie on the energy density curve $\mathcal{E}(\bar{\phi})$. In the non-degenerate case, while the true vacuum state $\bar{\phi} = 0$ is on the energy density curve $\mathcal{E}(\bar{\phi})$, the vacuum excitation state $\bar{\phi} = \phi_{vex}$ lies on the analytical continuation of $\mathcal{E}(\bar{\phi})$, denoted by $\mathcal{E}_a(\bar{\phi})$, as illustrated in Figure 1.

### 4.1 Non-degenerate Case $(b^2 < 3ac)$

We assume that at time $t = 0$, the system is in the vacuum excitation state $|\ >$ which satisfies

$$< |\ \phi(x)\ | > \ = \ \phi_{vex} \tag{4.1}$$

at every point $x$ in the volume $\Omega$. For convenience, let us take $\Omega$ to be a cube, which will be divided into $N$ smaller cubes, each of a linear size $L$, and all adjacent cubes are separated by a distance $\delta$. Hence,

$$\Omega \ = \ N(L + \delta)^3 \tag{4.2}$$

where $\delta$ is of the order of the microscopic length of the problem, but $L$ is much larger and may even be of a macroscopic dimension; e.g.,

$$\delta \ \sim \ O(a^{-\frac{1}{2}}) \ , \text{ or } \quad O(b^{-1})$$

and

$$L \gg \delta \quad . \tag{4.3}$$

Let $p(t)$ be the probability that at a later time $t$ the system is either in a state in which

$$< \left| \phi(x) \right| > \; = \begin{cases} 0 & \text{in one of the cubes } L^3 \\ \text{arbitrary} & \text{in the surface region } \sim O(L^2\delta) \\ \phi_{vex} & \text{outside} \end{cases} \tag{4.4}$$

or in states that differ from (4.4) by some additional high energy quantum excitations inside the cube $L^3$ that has been singled out. In the non-degenerate vacuum case, one has $\mathcal{E}_\alpha(\phi_{vex}) > \mathcal{E}(0)$ where $\mathcal{E}_\alpha$ denotes the analytical continuation of $\mathcal{E}$. These states can have the same energy as the initial state, provided

$$L^3 \mathcal{E}_\alpha(\phi_{vex}) \; = \; L^3 \mathcal{E}(0) \; + \; \text{excitation energy} \quad . \tag{4.5}$$

Since $L$ is $\gg O(a^{-\frac{1}{2}})$ or $O(b^{-1})$, there is a large number of such states that satisfy (4.5); their entropy is proportional to $L^3$. Thus, by using the standard calculation of transition rates, one finds

$$p(t) \; = \; 1 - \exp(-\lambda_L t) \tag{4.6}$$

where $\lambda_L \neq 0$, and, at fixed $L$ and $\delta$ the probability $p(t)$ is <u>independent</u> of $N$.

As shown in Appendix D, a lower bound in $\lambda_L$ can be easily estimated; we find for L sufficiently large

$$\ln \lambda_L \; > \; (-\kappa L^3) \tag{4.7}$$

where $\kappa$ is positive definite, and depends only on the renormalized constants a, b and c.

Since the N cubes are arranged to be physically separated from each other, they can be regarded as independent systems. For an initial state (4.1), the probability that at a later time t the system remains in the same state is

$$\left[1 - p(t)\right]^N \; = \; \exp\left(-N \lambda_L t\right) \tag{4.8}$$

which, at a fixed L, approaches zero as N (and therefore $\Omega$) becomes $\infty$. Thus, if the vacuum excitation state extends over an infinite volume, <u>its lifetime is zero.</u>

However, the lifetime of a vacuum excitation in a limited volume v is quite a different matter. Let us consider a finite volume v and a surface region s that surrounds v. The domain v + s is, of course, inside the bigger volume $\Omega$ of the entire quantum system; for simplicity, one may assume $\Omega$ to be infinite. Let the vacuum excitation be described by the state $|\,\text{vex}\,\rangle$ which satisfies

$$\langle \text{vex} \,|\, \phi(x) \,|\, \text{vex} \rangle \; = \; \begin{cases} \phi_{\text{vex}} & \text{in } v \\ 0 & \text{outside } v + s \\ \text{arbitrary, though smooth, inside } s. \end{cases} \tag{4.9}$$

Furthermore, we assume that in its rest system (i.e., $|\text{vex}>$ is of zero 3-momentum) the shape of $v$ is one in which the linear dimension is $\sim O(v^{\frac{1}{3}})$ in all directions. Thus, because of (1.6), the rest mass of $|\text{vex}>$ is

$$M_{vex} = v\,\mathcal{E}_a(\phi_{vex}) + \text{surface energy}\,. \tag{4.10}$$

Such a state can decay through meson emissions. There are two dominant modes of decay: one is via the surface contraction, and the other is via the decay law (4.8), provided that $v$ is sufficiently large. The latter resembles a "boiling" mechanism; we may first imagine that $v$ is divided into $n$ smaller volumes, $v = n(L+\delta)^3$, and then each smaller volume $L^3$ decays exponentially as $\exp(-\lambda_L t)$. Let $\tau_c$ and $\tau_b$ be, respectively, the time scales for surface contraction and for boiling. It is clear that

$$\tau_c \sim v^{\frac{1}{3}} \qquad \text{and} \qquad \tau_b \sim (n\lambda_L)^{-1}\,. \tag{4.11}$$

For $v$ small, the decay time is determined by $\tau_c$, and for $v$ sufficiently large by $\tau_b$. To have a rough idea of the critical volume size when $\tau_c \sim \tau_b$, we may use the lower bound (4.7) as an estimate of $\lambda_L$. As shown in Appendix D, this lower bound is derived by using the W.K.B. approximation; we may write

$$-\ln(\lambda_L \delta) \equiv P \sim 2L^3 \int \left[U(\phi) - U(\phi_{vex})\right]^{\frac{1}{2}} d\phi \tag{4.12}$$

in which $\delta$ is, as before, $\sim O(a^{-\frac{1}{2}})$ or $O(b^{-1})$, $U(\phi)$ is given by (1.2) and the integral extends from $\phi_{vex}$ to $\phi_0$ where $U(\phi_0) = U(\phi_{vex})$. Because $L$ is

$\gg \delta$, we expect $P$ to be quite large, and therefore at $\tau_b \sim \tau_c$ the critical volume $v_c$ should also be rather large. For example, if we arbitrarily assume $L \sim 10\delta$, $\delta \sim 10^{-13}$ cm and $P \sim 10^2$, then $v_c$ is $\sim (\text{mm.})^3$; the corresponding lifetime of the vacuum excitation state $|\text{vex}>$ is $\sim 3 \times 10^{-12}$ sec. Since the theory is Lorentz-invariant, such a state can acquire a nonzero momentum; of course, its shape would then undergo a Lorentz contraction, and its lifetime a time dilatation.

## 4.2 Degenerate Vacuum $(b^2 = 3ac)$

In this case, the system is invariant under the transformation

$$\bar{\phi} + \frac{b}{c} \rightarrow -(\bar{\phi} + \frac{b}{c}) \quad . \tag{4.13}$$

The states $\bar{\phi} = 0$ and $\bar{\phi} = -(2b/c)$ are therefore completely symmetrical with respect to each other. We observe that any classical path in the functional space $\phi(x)$ that connects these two states must pass through a potential barrier whose height is at least proportional to $\Omega^{\frac{2}{3}}$, where $\Omega$ is the volume of the entire system. The transition matrix element between these two states becomes zero as $\Omega$ approaches $\infty$. Consequently, in an infinite volume, the states $\bar{\phi} = 0$ and $\bar{\phi} = -(2b/c)$ are degenerate, and are both stable.

Next, we examine the lifetime of a vacuum excitation that extends over only a limited volume $v$ (but $\Omega$ is still $\infty$). Let $|\text{vex}>$ be such a vacuum excitation state defined by (4.9), where $\phi_{vex} = -(2b/c)$. In this case, the rest mass consists of only the surface energy, and the lifetime is determined completely by surface contraction. It is not possible to have "boiling" inside $v$, because of energy conservation.

Near the surface, "boiling" is possible, but then there is no clear distinction between that and surface contraction.

In both the degenerate and the non-degenerate cases, we see that the vacuum excitation can, in principle, extend over a domain of macroscopic sizes. In the degenerate case, there is no limit to its size; the larger its dimension is, the bigger its mass, but the smaller its width, and therefore the sharper is the definition of the state. In the non-degenerate case, the same holds only if the "boiling" mechanism can be neglected, and that gives an upper limit to its size.

## 5. Classical Solution

Some knowledge of the actual shape of the vacuum excitation state in space may be obtained by studying its classical solution; this is especially useful if its size may extend over a macroscopic region. For simplicity, we concentrate mainly on the degenerate case ($b^2 = 3ac$) in this section. With slight modifications, the method used below can be readily applied to the non-degenerate case ($b^2 \neq 3ac$) as well.

### 5.1 One Spatial Dimension

It is convenient to introduce the dimensionless variables:

$$x = a^{-\frac{1}{2}} \xi \quad , \quad t = a^{-\frac{1}{2}} \tau$$
$$\text{and} \qquad \phi = \frac{b}{c} (X - 1) \quad . \tag{5.1}$$

The wave equation for the degenerate case $b^2 = 3ac$ in a one-dimensional space becomes

$$- \frac{\partial^2 X}{\partial \tau^2} + \frac{\partial^2 X}{\partial \xi^2} + \tfrac{1}{2} X(1 - X^2) = 0 \quad . \tag{5.2}$$

We first examine the time-independent solution. From (5.2), it follows that if $\frac{\partial X}{\partial \tau} = 0$ then

$$\frac{dK}{d\xi} = 0 \tag{5.3}$$

where

$$K \equiv \tfrac{1}{2}\left(\frac{dX}{d\xi}\right)^2 - \frac{1}{8}(1-X^2)^2 \quad . \tag{5.4}$$

Thus, if we regard $\xi$ as a fictitious "time", the problem becomes identical to one in elementary mechanics, in which there is a point particle at $X$ moving in a potential

$$W \equiv -\frac{1}{8}(1-X^2)^2 \tag{5.5}$$

and $K$ is the total energy of the particle. The explicit solution $X = X(\xi)$ can then be readily obtained.

To illustrate the different types of solutions in this problem, we may consider, for example, the special case $K = 0$. The solutions are

$$X = \pm 1 \tag{5.6}$$

and

$$X = \pm \tanh \tfrac{1}{2}(\xi - \xi_0) \tag{5.7}$$

where $\xi_0$ is a constant. In terms of the mechanical analog, (5.6) is the solution that the particle is at one of the two peaks of $W$, and (5.7) is the solution such that the particle goes from one peak to the other. In the field theory problem, the two solutions in (5.6) represent simply the two degenerate vacuum states $\bar{\phi} = 0$ and $\bar{\phi} = -(2b/c)$. The solution in (5.7) gives the details of the transition from $\bar{\phi} = 0$ at, say, $x = +\infty$ to $\bar{\phi} = -(2b/c)$ at $x = -\infty$.

Through a Lorentz transformation, the solution (5.7) can be easily transformed to one in which the transition region moves with a velocity $u$. The explicit form is

$$X = \pm \tanh \theta \tag{5.8}$$

where

$$\theta = \tfrac{1}{2}(1 - u^2)^{-\frac{1}{2}} \left[ \xi - u\tau + \text{constant} \right] .$$

5.2 Three-Dimensional Case

For simplicity, we consider only the spherically symmetrical solution. Again, we introduce the dimensionless variables

$$r = a^{-\frac{1}{2}} \rho \quad , \qquad t = a^{-\frac{1}{2}} \tau$$

and

$$\phi = \frac{b}{c}(X - 1) \quad . \tag{5.9}$$

For the degenerate case $(b^2 = 3ac)$, the wave equation becomes

$$-\frac{\partial^2 X}{\partial \tau^2} + \frac{1}{\rho^2} \frac{\partial}{\partial \rho}\left(\rho^2 \frac{\partial X}{\partial \rho}\right) + \tfrac{1}{2} X(1 - X^2) = 0 \quad . \tag{5.10}$$

For the time-independent solution $\frac{\partial X}{\partial \tau} = 0$, one has now, instead of (5.3),

$$\frac{dK}{d\rho} = -\frac{2}{\rho}\left(\frac{dX}{d\rho}\right)^2 \tag{5.11}$$

where, as before,

$$K = \tfrac{1}{2}\left(\frac{dX}{d\rho}\right)^2 - \frac{1}{8}(1 - X^2)^2 \quad . \tag{5.12}$$

Again, we may consider the mechanical analog by regarding $\rho$ as the "time" and $X$ as the "position" of a particle. The "potential" $W$ is again given by (5.5). But now because

$$\frac{dK}{d\rho} \leqq 0 \ , \tag{5.13}$$

the particle is in a dissipative system, with a "time"-dependent frictional force. The motion of the particle can be discussed in the standard way[9] by plotting the $K$ = constant contours in the phase space (with $X$ and $\frac{dX}{d\rho}$ as the coordinates). Since a regular solution at $\rho = 0$ implies that $X(0)$ is finite and $\left(\frac{dX}{d\rho}\right)_{\rho=0}$ is zero, at $\rho = 0$, the trajectory must begin at a point on the real axis (i.e., $\frac{dX}{d\rho} = 0$) in the phase space. As $\rho$ increases, because of (5.13), the value of $K$ along the trajectory must keep on decreasing. From Figure 4, one sees that the $K = 0$ contour divides the entire phase space into one closed region $\mathfrak{R}$ and four open regions. Thus, depending on the initial value $X(0)$, there are three types of solutions: (i) Stationary solution. If $X(0) = 1$ or $-1$, then at all $\rho \geqq 0$

$$X(\rho) = 1 \ , \quad \text{or} \quad -1 \ . \tag{5.14}$$

(ii) Runaway solution. For $X(0) > 1$, or $< -1$, the trajectory in the phase space moves toward points at infinity as $\rho$ increases. (iii) Spiral solution. If $-1 < X(0) < 1$, the trajectory lies within the closed region $\mathfrak{R}$ bounded by the $K = 0$ contour. Inside $\mathfrak{R}$, the minimum $K$ is at the origin. As illustrated by the dashed curve in Figure 4, a typical trajectory would begin at a point on the real axis at $\rho = 0$, then spiral in, and

eventually approach the origin as $\rho \to \infty$ .

Returning to the field-theory problem, one sees that the two stable solutions given by (5. 14) correspond to the two degenerate vacuum states $\bar{\phi} = 0$ and $\bar{\phi} = -(2b/c)$ . Both the runaway solution and the spiral solution have a field-energy content $\int d^3r \left[\frac{1}{2}(\nabla\phi)^2 + U(\phi)\right]$ that is infinite. Thus, they are unphysical. This situation is quite different from the one-dimensional case; as shown in the previous section, there is a time-independent solution (5. 7) in which $X$ is not a constant, and the solution has a finite field-energy. In three dimensions, a similar transition from $X \cong -1$ at, say, $\rho << R$ to $X = +1$ at $\rho >> R$ gives rise to a surface energy which can always be reduced by decreasing $R$ . Thus, such a solution cannot be stable (i.e., time-independent) as in the one-dimensional case.

## 5.3 Constant External Source

It is therefore of interest to examine the three-dimensional time-independent classical solutions which may exist in the presence of an external source $J(x)$ . For example, we may assume that the spin 0 field $\phi(x)$ is of parity $+1$ , and interacts with a spin $\frac{1}{2}$ nucleon field $\psi$ through a scalar coupling $-g\,\psi^\dagger\gamma_4\,\psi\phi$ . The Lagrangian density is given by

$$\mathcal{L} = -\tfrac{1}{2}\left(\frac{\partial\phi}{\partial x_\mu}\right)^2 - U(\phi) - \psi^\dagger\gamma_4\left(\gamma_\mu\,\frac{\partial}{\partial x_\mu} + m_N\right)\psi$$

$$- g\,\psi^\dagger\gamma_4\,\psi\phi + \text{counter terms} \qquad (5.15)$$

where $U(\phi)$ is given by (1. 2), $m_N$ is the physical mass of the nucleon, $\psi^\dagger$ is the

Hermitian conjugate of $\psi$ and $g$ the renormalized coupling constant. The wave equation is now of the form

$$\frac{\partial^2 \phi}{\partial x_\mu^2} - \frac{dU}{d\phi} - J = 0 \qquad (5.16)$$

where (neglecting the counter term)

$$J = g \psi^\dagger \gamma_4 \psi \ .$$

In this section, we shall assume that in regions occupied by nuclear matter, the source $J$ is a constant. Physically, we may assume either $g$ weak or $m_N$ large, so that

$$m_N^2 \gg (g \phi_{vex})^2 \ . \qquad (5.17)$$

[The case $m_N^2 \lesssim (g \phi_{vex})^2$ will be considered in the next section.] Thus, when $\phi$ changes from 0 to $O(\phi_{vex})$, the coupling term $g \phi \psi^\dagger \gamma_4 \psi$ remains much smaller than the nucleon-mass term $m_N \psi^\dagger \gamma_4 \psi$. The perturbation on $\psi$ due to the variation of $\phi$ may therefore be neglected. So far as the classical solution is concerned, we may then regard $J(x)$ as a given function. For definiteness, we consider $J(x)$ to resemble the nucleon distribution in, say, a spherical heavy nucleus; it will be assumed to be time-independent and of the form

$$J(x) = \begin{cases} 0 & \text{if } \rho < R \\ (\frac{ab}{c})\, j & \text{if } \rho > R \end{cases}$$

where $\rho$ is defined by (5.9), $R$ and $j$ are both dimensionless constants.

By using the dimensionless variables introduced in (5.9), we find that for the degenerate vacuum case ($b^2 = 3ac$), the time-independent spherically symmetric equation is, as before,

$$\frac{1}{\rho^2}\frac{d}{d\rho}\left(\rho^2\frac{dX}{d\rho}\right) + \tfrac{1}{2}X(1-X^2) = 0 \qquad (5.18)$$

in the outside region $\rho > R$; it is

$$\frac{1}{\rho^2}\frac{d}{d\rho}\left(\rho^2\frac{dX}{d\rho}\right) + \tfrac{1}{2}X(1-X^2) = j \qquad (5.19)$$

in the inside region $\rho < R$. At $\rho = R$, the outside and inside solutions are joined together so that $X$ and $\frac{dX}{d\rho}$ are both continuous. The solution is then determined by requiring $X$ to be regular at the origin and at infinity.

The solutions that we are interested in are those for $R$ large and in which $X$ is nearly a constant either inside $\rho = R$, or outside; only near the boundary $\rho \cong R$ does $X$ have any significant variation. In order to have the "true" vacuum $\phi = 0$ at infinity, we require that in the outside region $X \to 1$, as $\rho \to \infty$; the next term in the asymptotic expansion of $X$ is then exhibited in:

$$X \to 1 - \lambda\rho^{-1}\exp(-\rho) \qquad (5.20)$$

where $\lambda$ is a constant. In the inside region, we require as $\rho \to 0$,

$$X \to X_0 + \epsilon\rho^{-1}\sinh(\kappa\rho) \qquad (5.21)$$

where $\epsilon \ll 1$, $X_0$ satisfies

$$X_0(1 - X_0^2) = 2j \tag{5.22}$$

and

$$\kappa^2 = \tfrac{1}{2}(3X_0^2 - 1) \quad . \tag{5.23}$$

It can be readily verified that in the outside region, the asymptotic solution (5.20) satisfies the differential equation (5.18) to first order in $(X - 1)$; similarly, in the inside region, the corresponding limiting solution (5.21) satisfies (5.19) to first order in $(X - X_0)$. The exact determination of these parameters $\lambda$ and $\epsilon$ in terms of $j$ and $R$ is rather involved, but some of the general characteristics can be derived without detailed calculations.

For $j^2 < \frac{1}{27}$, Eq. (5.22) has three real roots $X_0 = X_\alpha$, $X_\beta$ and $X_\gamma$, given by

$$X_\alpha = \frac{2}{\sqrt{3}} \cos\left(\frac{\delta}{3} + \frac{2\pi}{3}\right) \quad , \quad X_\beta = \frac{2}{\sqrt{3}} \cos\left(\frac{\delta}{3}\right)$$

$$X_\gamma = \frac{2}{\sqrt{3}} \cos\left(\frac{\delta}{3} + \frac{4\pi}{3}\right) \quad \text{and} \quad \cos\delta = -3\sqrt{3}\, j \quad . \tag{5.24}$$

We choose $\pi \geqq \delta \geqq 0$, and therefore $X_\alpha \leqq X_\gamma \leqq X_\beta$. By following the same argument given in the previous section, one can show that for $j < 0$ there is no solution which satisfies the desired boundary conditions (5.20) and (5.21). At $j = 0$, the three roots are $X_\alpha = -1$, $X_\beta = +1$ and $X_\gamma = 0$, but there is only one solution that

satisfies the boundary conditions (5.20) and (5.21): $\chi(\rho) = 1$ at all $\rho$.

At a fixed $R$, as $j$ increases gradually from zero, the inside solution assumes (except near the surface $\rho = R$) the form (5.21) with $\chi_0 = \chi_\beta$. Because of the continuity condition at $\rho = R$, the value of $\epsilon$ is $\sim O(e^{-\kappa R})$. For $R \gg 1$, which is the case of physical interest for the classical solution, $\epsilon$ is exceedingly small. Thus, $\chi \cong \chi_\beta < 1$ near the origin. At larger $\rho$, the inside solution increases very slowly. It makes a rapid rise only when near the surface $\rho = R$. At the surface, it connects with the outside solution, and then approaches 1 asymptotically as $\rho \to \infty$. According to (5.22), as $j$ increases beyond $j = \dfrac{1}{3\sqrt{3}}$, the root $\chi_0 = \chi_\beta$ ceases to exist, and therefore the solution disappears. Physically, this means that inside $\rho < R$, as $j$ increases adiabatically from zero, the state shifts from $\phi(x) = 0$ to $\phi(x) < 0$, until $j$ reaches the value at point B in Figure 3. Beyond that, $\phi(x)$ has to make a jump to a completely different solution which represents the vacuum excitation state.

To obtain this other solution, let us first consider the case $R \gg 1$ and $j \ll 1$. We assume that the solution is approximately given by (5.21) in the region $\rho < (R-d)$ where $\chi_0 = \chi_\alpha \cong -1$ and $d \sim O(1)$. In the region $\rho > (R+d)$, we assume that the solution is approximately given by (5.20). In the transition region $(R-d) < \rho < (R+d)$, we may neglect both $R^{-1}$ and $j$ as a zeroth approximation; thus, according to (5.7), we have

$$\chi \cong \tanh \tfrac{1}{2}(\rho - \rho_0) \tag{5.25}$$

where $\rho_0$ lies within the transition region. From the continuity condition, it follows

that $\epsilon \sim O(e^{-R})$, and therefore $X \cong -1$ in the region $\rho < (R-d)$. Similarly, we find $X \cong +1$ in the region $\rho > R+d$. By multiplying (5.18) and (5.19) by $\frac{dX}{d\rho}$ and then integrating over all space, we find

$$j\,\delta X = 2\int \rho^{-1}\left(\frac{dX}{d\rho}\right)^2 d\rho \tag{5.26}$$

where

$$\delta X = X(R) - X(0) \ . \tag{5.27}$$

In terms of the mechanical analog discussed in the previous section, (5.26) implies simply that the energy dissipated by the "frictional force" equals the work done by the "external force" $j$. To evaluate approximately the "energy dissipation", we need only to consider the transition region. By using (5.25), we find the right-hand side of (5.26) to be approximately given by $\frac{4}{3R}$. Since for $j \ll 1$, $\delta X$ is $< 2$, we derive the approximate condition

$$j > \frac{2}{3R} \tag{5.28}$$

in order to have the vacuum excitation solution inside $\rho = R$.

Next, we examine its field-energy content

$$4\pi \int H \rho^2 d\rho$$

where $H$ is

$$H = \tfrac{1}{2}\left(\frac{dX}{d\rho}\right)^2 + \tfrac{1}{8}(1-X^2)^2 + \begin{cases} jX & \text{for } \rho < R \\ 0 & \text{for } \rho > R \end{cases} .$$

By using the above solution which is valid for $R \gg 1$ and $j \ll 1$, we find that to first order in $j$ the integral of the Hamiltonian density $H$ in the inside region, $\rho < R-d$, is given by

$$(4\pi) \int_0^{R-d} j\chi\rho^2 d\rho \cong -\frac{4\pi}{3} R^3 j \quad .$$

The energy content in the transition region is approximately given by

$$4\pi R^2 \int_{R-d}^{R+d} \left[ \tfrac{1}{2} \left( \frac{d\chi}{d\rho} \right)^2 + \tfrac{1}{8} (1-\chi^2)^2 \right] d\rho \cong \frac{8\pi}{3} R^2 \quad .$$

To the same order, we may neglect the energy content in the outside region $\rho > (R+d)$. The total field energy content is therefore

$$\frac{4\pi}{3} R^2 (2 - Rj) \quad . \tag{5.29}$$

This is to be compared with the approximate energy content

$$\frac{4\pi}{3} R^3 j \tag{5.30}$$

of the other solution ($\chi \cong \chi_\beta \sim 1$ inside $\rho < R$). Thus, for $R \gg 1$, by comparing (5.29) with (5.30), we find that the vacuum excitation solution has a lower energy if $j > \frac{1}{R}$.

To summarize: For $R \gg 1$, as $j$ gradually increases from 0, the solution changes continuously from $X = 1$ everywhere to one in which $X \cong X_\beta \lesssim 1$ in the inside region $\rho \ll R$, but $X$ remains $\cong +1$ in the outside region $\rho \gg R$. As $j$ becomes larger than $\frac{2}{3R}$, there appears another solution, called the vacuum excitation solution, in which $X \cong X_\alpha < -1$ for $\rho \ll R$, though $X$ is still $\cong +1$ for $\rho \gg R$. If $j$ becomes $> \frac{1}{R}$, then the vacuum excitation solution has a lower energy. When $j$ exceeds $\frac{1}{3\sqrt{3}}$, the vacuum excitation becomes the only form of time-independent solution.

## 5.4 External Source (Free Nucleon Gas)

We now turn to the case in which the coupling constant $g$ in (5.15) is assumed to be sufficiently strong, so that (5.17) may not hold. We recall that in the "true" vacuum, because of our convention (1.3), $\bar{\phi} = 0$; by definition, the nucleon mass is $m_N$. However, in states with $\bar{\phi} \neq 0$, the nucleon mass is $m_N + g\bar{\phi}$. In discussing the classical equation, if the solution $\phi(x)$ is slowly varying, we may expect $\phi(x)$ to replace locally the role of $\bar{\phi}$ in the quantum mechanical treatment. Thus, the "effective" mass of the nucleon becomes $m_N + g\phi$, which in the present case may be quite different from $m_N$. For definiteness, let us again consider the example of a heavy nucleus. Inside the nucleus, we have

$$< \psi^\dagger \psi > \; = \; n \tag{5.31}$$

where $n$ is the nucleon density, and $< >$ denotes the expectation value. However,

as we shall see, when g is strong (or relatively speaking, $m_N$ not too large), unlike (5.17), $< \psi^\dagger \gamma_4 \psi > \neq$ constant and must depend on $\phi$.

To discuss the classical solution of the spin 0 field, we shall assume the nucleons to be approximately described by a degenerate Fermi distribution, characterized by a maximum Fermi momentum $k_F$. In the simple example of an equal number of protons and neutrons, $k_F$ is given by

$$k_F = (3\pi^2 n/2)^{\frac{1}{3}} \quad . \tag{5.32}$$

Since the classical solution $\phi(x)$ is expected to be slowly varying inside the nucleus, one may treat $m_N + g\phi(x)$ as the "effective" mass of the nucleon at $x$; the density of the kinetic energy of nucleons is therefore given by

$$\begin{aligned} U_N &= \frac{2}{\pi^2} \int_0^{k_F} k^2 (k^2 + M^2)^{\frac{1}{2}} \, dk \\ &= (2\pi^2)^{-1} \left\{ k_F (k_F^2 + M^2)^{\frac{1}{2}} (k_F^2 + \tfrac{1}{2} M^2) - \tfrac{1}{2} M^4 \ln \frac{k_F + (k_F^2 + M^2)^{\frac{1}{2}}}{M} \right\} \end{aligned} \tag{5.33}$$

where $M^2 = (m_N + g\phi)^2$. The nuclear density n is determined both by the usual short-range nuclear forces (generated through the exchange of high frequency virtual mesons) and by the long-range "classical" potential $\phi(x)$ (which, in the time-independent solution, is of zero-frequency). In the following, we shall consider two models: (i) the free gas model, to be discussed in this section, and (ii) the incompressible fluid model, which will be discussed in the next section. The actual physical

situation should lie somewhere in between these two extreme possibilities.

Free Nucleon Gas Model

In this model, we neglect all short-range nuclear forces, as well as the electromagnetic interaction between nucleons. The nucleons are treated as a free degenerate Fermi gas moving in a classical field $\phi(x)$. To derive the time-independent field equation, we consider the minimum of the field energy $E$, defined by

$$E \equiv \int \left[ \tfrac{1}{2} (\nabla \phi)^2 + U_\phi + U_N \right] d^3r \ , \tag{5.34}$$

but subject to the constraint that the total number of nucleons $N$ is a constant, where for a system of equal number of neutrons and protons,

$$N = \frac{2}{3\pi^2} \int k_F^3 \, d^3r \ , \tag{5.35}$$

$U_N$ is given by (5.33) and $U_\phi$ is given by (1.2); i.e.,

$$U_\phi = \tfrac{1}{2} a \phi^2 + (3!)^{-1} b \phi^3 + (4!)^{-1} c \phi^4 \ . \tag{5.36}$$

By setting, at constant $k_F$, the variational derivative of $E$ with respect to $\phi$ equal to zero, we derive

$$- \nabla^2 \phi + \frac{d}{d\phi} U_\phi + \left( \frac{\partial}{\partial \phi} U_N \right)_{k_F} = 0 \ . \tag{5.37}$$

Next, let us consider the variation of $E$ with respect to $k_F$, at constant $\phi$ and under the constraint (5.35). By using the standard Lagrangian multiplier method, we find that in order to have $E$ minimum,

$$k_F^2 \left[ (k_F^2 + M^2)^{\frac{1}{2}} - \text{constant} \right] = 0 \tag{5.38}$$

where the constant is the Lagrangian multiplier. Thus, at any point in space, either there is no nuclear matter, hence $k_F = 0$, or since $M = m_N + g\phi$, $k_F$ is related to $\phi$ by

$$k_F^2 + (m_N + g\phi)^2 \equiv \omega^2 m_N^2 = \text{constant} \tag{5.39}$$

which implies that the top energy of the degenerate Fermi sea is a constant. Together, (5.37) and (5.38) determine the classical time-independent equation for $\phi$.

The most remarkable consequence of the above field equation is the possibility that it may have solutions in which the $N$ nucleons can be bound together in a region of finite and non-zero volume, even though the nucleons are treated as free gas particles without any short range forces. Furthermore, these solutions exhibit typical "saturation" properties; i.e., for $N$ sufficiently large, the volume is proportional to $N$ and the binding energy per nucleon is independent of $N$. In such solutions, the classical field $\phi \to 0$ at infinity, so that, in accordance with our convention (1.3), we have the usual vacuum at infinity. However, the constant $\omega$ in (5.39) is chosen to be $< 1$, so that there can be a finite volume in space in which $g\phi$ is negative and $< -m_N(1 - \omega)$. The nuclear matter will be confined in this volume, whose boundary

is defined by

$$g\,\phi(x) \;=\; -\,m_N(1-\omega) \;<\; 0 \quad . \tag{5.40}$$

As we shall see, if $g$ is sufficiently large, one has

$$m_N + g\,\phi \;\cong\; 0 \tag{5.41}$$

inside the bound volume, except in a small region near the boundary; therefore, because of (5.39), inside the volume

$$k_F \;\cong\; \omega\, m_N \quad ; \tag{5.42}$$

i.e., the nuclear density $n \cong 2(3\pi^2)^{-1}(\omega\, m_N)^3$ is also nearly a constant inside. Furthermore, because of (5.41), the "effective" mass of the nucleon is $\cong 0$. Thus, the field energy $E$ for such a bound solution is given by

$$E \;=\; \left[\frac{(\omega\, m_N)^4}{2\pi^2} + U_\phi(-m_N/g)\right] \cdot \Omega_N \;+\; \text{surface energy}$$

where $\Omega_N$ denotes the volume of the bound solution and $U_\phi(-m_N/g)$ is the value of $U_\phi$ at $\phi = -m_N/g$. Because of (5.35), $k_F$ is $\propto \Omega_N^{-\frac{1}{3}}$. Therefore, if one neglects the surface energy, the minimum of $E$ occurs at $(\partial E/\partial \Omega_N) = 0$; i.e.,

$$(\omega\, m_N)^4 \;=\; 6\pi^2\, U_\phi(-m_N/g) \quad . \tag{5.43}$$

By using (5.35), one finds

$$N = 2(3\pi^2)^{-1}(\omega m_N)^3 \Omega_N + O(\Omega_N^{\frac{2}{3}}) \quad .$$

The minimum energy $E$ of the bound solution is given by

$$N^{-1}E = \omega m_N + O(N^{-\frac{1}{3}}) \quad . \tag{5.44}$$

This is to be compared with the lowest energy $N m_N$ of the unbound solution [in which $\phi = 0$ and $k_F = 0$ everywhere, but one retains (5.35) by having the particles at infinity]. Now since, according to (5.36), $U_\phi = 0$ at $\phi = 0$, the bound solution has a lower energy than the unbound solution, provided $g$ is sufficiently large so that[10]

$$6\pi^2 U_\phi(-m_N/g) < m_N^4 \quad , \tag{5.45}$$

and therefore $\omega < 1$; in addition, $N$ must be sufficiently large so that the surface energy can be neglected. The binding energy per nucleon is $(1-\omega) m_N$.

We emphasize that, unlike the other topics discussed in this paper, the existence of this rather unusual type of heavy "nucleus" is independent of the existence of another local minimum in $U_\phi$ (besides $\phi = 0$); it may occur even if the $\phi^3$-coupling $b = 0$.

To illustrate more explicitly the details of such bound solutions, let us consider the degenerate vacuum case $b^2 = 3ac$. In addition, for simplicity we shall also assume

$$m_N = g\,b/c \tag{5.46}$$

so that both $U_\phi$ and $U_N$ are symmetric under the transformation (3.7): $\phi + \frac{b}{c} \to -(\phi + \frac{b}{c})$. By using the dimensionless variables introduced in (5.9), one has

$$r = a^{-\frac{1}{2}}\rho \qquad \text{and} \qquad X = 1 + (g\phi/m_N) \quad . \tag{5.47}$$

Let $\rho = R$ be the boundary of a spherically symmetric solution, representing a heavy nucleus. Because of (5.37)-(5.39), the corresponding time-independent equation is given by

$$\frac{1}{\rho^2}\frac{d}{d\rho}\left(\rho^2 \frac{dX}{d\rho}\right) + \tfrac{1}{2}X(1-X^2) = 0 \qquad \text{for} \quad \rho > R \tag{5.48}$$

$$= j_N \qquad \text{for} \quad \rho < R \tag{5.49}$$

where

$$j_N = 2\beta X\left\{(\omega^2 - X^2)^{\frac{1}{2}}\omega - \tfrac{1}{2}X^2 \ln\left[\frac{\omega + (\omega^2 - X^2)^{\frac{1}{2}}}{X}\right]^2\right\}, \tag{5.50}$$

$$\beta = 3g^4/(2\pi^2 c) \tag{5.51}$$

and

$$(k_F/m_N) = (\omega^2 - X^2)^{\frac{1}{2}} \quad . \tag{5.52}$$

The boundary $\rho = R$ is determined by

$$X(R) = \omega \quad .$$

As $\rho \to \infty$, the asymptotic behavior of $X$ is given by (5.20),

$$X \to 1 - \lambda \rho^{-1} \exp(-\rho) \tag{5.53}$$

where $\lambda$ is a constant. As $\rho \to 0$, we have

$$\chi \to \epsilon \rho^{-1} \sinh \kappa\rho \tag{5.54}$$

where

$$\kappa^2 = 2\beta\omega^2 - \tfrac{1}{2} \tag{5.55}$$

which is assumed to be $>0$. Both $\chi$ and $\left(\frac{d\chi}{d\rho}\right)$ are continuous at $\rho = R$. Therefore, the constant $\epsilon$ is $O(e^{-\kappa R})$; consequently, except when near the boundary, inside the nucleus $\chi$ is $\sim O(e^{-\kappa R}) \cong 0$, provided that $R$ is large.

Let $\chi_{out}$ and $\chi_{in}$ be, respectively, the solutions of (5.48) and (5.49) that satisfy the conditions (5.53) and (5.54). To study how these two solutions can be connected at $\rho = R$, we note that at $\rho \gg 1$, $\rho^{-2} \frac{\partial}{\partial\rho}\left(\rho^2 \frac{\partial}{\partial\rho}\chi\right) \cong \frac{\partial^2\chi}{\partial\rho^2}$. Thus, when $R$ is sufficiently large, (5.48) implies that at $\rho = R$ the outside solution $\chi_{out}$ satisfies

$$\frac{d\chi_{out}}{d\rho} = \tfrac{1}{2}(1 - \chi_{out}^2) , \tag{5.56}$$

which can be easily derived by following the same steps leading to (5.4). Similarly, from (5.49) one concludes that in the transition region near the boundary,

$$R \geqq \rho \geqq (R - d) \gg 1 , \tag{5.57}$$

the inside solution $\chi = \chi_{in}$ satisfies

$$\tfrac{1}{2}\left(\frac{dX}{d\rho}\right)^2 - \tfrac{1}{8}(1-X^2)^2 - \int j_N\, dX = \text{constant} \qquad (5.58)$$

where

$$\int j_N\, dX = \frac{1}{6}\beta\left[\omega(5X^2 - 2\omega^2)(\omega^2 - X^2)^{\frac{1}{2}} - 3X^4 \ln\frac{\omega + (\omega^2 - X^2)^{\frac{1}{2}}}{X}\right] . \qquad (5.59)$$

The width d of the transition region (5.57) is $\sim O(1)$; it is chosen such that at $\rho = R-d$, $X_{in}$ and $\frac{dX_{in}}{d\rho}$ are $\cong 0$. Since at $\rho = R$, $X_{in} = \omega$, therefore (5.59) is zero; we obtain for R sufficiently large, at $\rho = R$

$$\frac{dX_{in}}{d\rho} = \left[\frac{1}{12}(8\beta+3)X_{in}^2 - \tfrac{1}{2}\right]^{\frac{1}{2}} X_{in} . \qquad (5.60)$$

The intersection of (5.56) and (5.60) determines X and $\frac{dX}{d\rho}$ at $\rho = R$. We find

$$X(R) = \omega = \left(\frac{3}{8\beta}\right)^{\frac{1}{4}} , \qquad (5.61)$$

provided that R is sufficiently large. This result, of course, agrees with (5.43). If we neglect the surface energy, then the binding energy per nucleon is

$$m_N(1-\omega) . \qquad (5.62)$$

As we shall see in Section 6, in the $\sigma$-model the constant $\beta$ is given by $\beta \cong \frac{g^2}{2\pi^2}\left(\frac{m_N}{m_\sigma}\right)^2$. [See Eq. (6.13).] This leads to a value $\beta \cong 10$ if $(4\pi)^{-1} g^2 \cong 15.7$ and $m_\sigma \cong m_N$. The corresponding value of $\omega$ is $\cong 0.44$.

In Figure 5, the two solid curves, labeled "outside ($R = \infty$)" and "inside ($R = \infty$)" refer respectively to (5.56) and (5.60) with $\beta = 10$. These are to be compared with the dashed curves for $R = 10$, determined by the numerical solutions of (5.48) and (5.49). As a further illustration, the numerical solution of $X(\rho)$ is plotted in Figure 6 for $R = 20$ and $\beta = 10$; the corresponding value of $N$ is $\cong 210$ and that of $\omega$ is $\cong 0.46$, which is to be compared with the asymptotic value $\omega \cong 0.44$ if $R$ is $\infty$.

## 5.5 External Source (Incompressible Nucleon Fluid)

In this model, we assume the short-range nuclear force to be so strong that the nuclear density $n$ is a constant. The nuclear matter resembles an incompressible fluid. Thus, if we retain the approximation that the nucleon density is still related to the Fermi momentum $k_F$ by (5.32) and that the kinetic energy of the nucleons remains given by (5.33), then the time-independent equation for $\phi$ is

$$- \nabla^2 \phi + \frac{d}{d\phi} U_\phi = 0 \tag{5.63}$$

outside the nucleus, and

$$- \nabla^2 \phi + \frac{d}{d\phi} U_\phi + \left( \frac{\partial}{\partial \phi} U_N \right)_{k_F} = 0 \tag{5.64}$$

inside the nucleus, which is the same as (5.37), except that instead of (5.38) we have now

$$k_F = \text{constant} \quad . \tag{5.65}$$

To illustrate the main feature of the model, let us consider again the degenerate vacuum case $b^2 = 3ac$, and let us assume that (5.46) holds. For the spherically symmetric case, in terms of the dimensionless variables $\rho$ and $X$, introduced in (5.47), Eqs. (5.63) and (5.64) become

$$\frac{1}{\rho^2}\frac{d}{d\rho}\left(\rho^2\frac{dX}{d\rho}\right) + \tfrac{1}{2}X(1-X^2) = 0 \qquad \text{for } \rho > R \qquad (5.66)$$

$$= \frac{d}{dX}V_N \qquad \text{for } \rho < R \qquad (5.67)$$

where

$$V_N(X) = \beta\left\{a(a^2+X^2)^{\frac{1}{2}}(a^2+\tfrac{1}{2}X^2) - \tfrac{1}{4}X^4 \ln\left[\frac{a+(a^2+X^2)^{\frac{1}{2}}}{X}\right]^2\right\}, \qquad (5.68)$$

$\rho = R$ is the radius of the nucleus and $\alpha$, $\beta$ are both constants, given by

$$\alpha = k_F/m_N \qquad \text{and} \qquad \beta = 3g^4/(2\pi^2 c) \ . \qquad (5.69)$$

The field energy of the system is given by

$$E = E_{out} + E_{in} \qquad (5.70)$$

where apart from a common multiplicative factor

$$E_{out} \propto \int_R^\infty \rho^2 d\rho \left[\tfrac{1}{2}\left(\frac{dX}{d\rho}\right)^2 + \tfrac{1}{8}(1-X^2)^2\right], \qquad (5.71)$$

$$E_{in} \propto \int_0^R \rho^2 d\rho \left[ \tfrac{1}{2}\left(\frac{dX}{d\rho}\right)^2 + V(X) \right] , \tag{5.72}$$

and

$$V(X) = \tfrac{1}{8}(1 - X^2)^2 + V_N(X) - V_N(1) \tag{5.73}$$

in which the constant term $- V_N(1)$ is arbitrarily added, such that for the true vacuum $\phi = 0$, $X = 1$, one has $V(1) = 0$. Different from the previous free gas model, the nuclear radius $R$ is pre-determined by the given constant $n$ and the given number of nucleons. By varying $E_{out}$ and $E_{in}$ independently, we derive the field equations (5.66) and (5.67).

Outside the nucleus, the solution has the same form as that in the previous section; e.g., the asymptotic solution remains given by (5.53) as $\rho \to \infty$. However, as will be analysed, the solution $X$ inside the nucleus changes its character depending on the physical parameters. In the weak coupling limit, as expected, the equation becomes identical to that in the constant current model, discussed in Section 3.3. Similar behavior also occurs in the low nucleon density limit, even though the coupling constant $g$ may be strong. But when the nucleon density is sufficiently high and $g$ strong, the solution resembles that in the free gas model.

We first observe that as $g \to 0$, the minimum of $V$ is at $X = \pm 1 + O(g)$; therefore, to zeroth order in $g$, the current

$$j \equiv \frac{dV_N}{dX} = 2\beta \left\{ \alpha(\alpha^2+1)^{\frac{1}{2}} - \ln\left[\alpha + (\alpha^2+1)^{\frac{1}{2}}\right] \right\} \tag{5.74}$$

is a constant inside the nucleus. Equation (5.67) reduces to the previous Eq. (5.19).

Next, we consider the case where $g$ is strong, but the nucleon density $n \to 0$, and therefore $a$ also $\to 0$. At $X = 0$, one has $\frac{dV}{dX} = 0$ and $\frac{d^2V}{dX^2} = 2\beta a^2 - \frac{1}{2}$; consequently as $a \to 0$, the point $X = 0$ is a local maximum of $V$. The minimum of $V$ remains at $X \cong \pm 1$; the solution then retains the character of the constant current model. However, when $a$ increases to

$$2\beta a^2 > \tfrac{1}{2} \quad ,$$

the point $X = 0$ becomes a local minimum of $V$. When the nucleon density becomes sufficiently high, $X = 0$ becomes the absolute minimum of $V$. Thus, it resembles the free gas model when $g$ is strong and nuclear density is sufficiently high. [This is in contrast to the situation in the constant current model, in which $X = 0$ is always the local maximum of the field-energy.] The corresponding solution inside the nucleus can be readily obtained by using (5.67).

As $\rho \to 0$, the solution satisfies

$$X \to \epsilon \rho^{-1} \sinh(\kappa\rho) \tag{5.75}$$

where

$$\kappa^2 = 2\beta a^2 - \tfrac{1}{2} \quad . \tag{5.76}$$

Because $X$ is continuous at $\rho = R$, and because outside the nucleus, according to (5.53), $X$ is $\leqq 1$, one finds that $\epsilon$ is $\sim O(e^{-\kappa R})$. Thus, if $R$ is sufficiently large, for the most part inside the nucleus, the value of $X$ is near zero. As $\rho$ approaches $R$, $X$ begins to increase. If one neglects $O(R^{-1})$, then one has for

$\rho$ near R but inside the nucleus,

$$\tfrac{1}{2}\left(\frac{dX}{d\rho}\right)^2 - V(X) \cong -V(0) \tag{5.77}$$

for $\rho$ near R and outside the nucleus, one has

$$\tfrac{1}{2}\left(\frac{dX}{d\rho}\right)^2 - \tfrac{1}{8}(1-X)^2 \cong 0 \quad . \tag{5.78}$$

Consequently, at $\rho = R$, X satisfies

$$V_N(X) \cong \beta\alpha^4 \quad . \tag{5.79}$$

In order for $X = 0$ to be the absolute minimum of V, we must have $V(0) < V(1)$ ; i.e.,

$$V_N(1) - \beta\alpha^4 > \tfrac{1}{8} \quad . \tag{5.80}$$

If $\beta$ is $>> 1$, this inequality can be satisfied for a relatively small $\alpha$, and therefore also a relatively low nuclear density. Since for $\alpha$ small, $V_N(1) \cong \frac{4}{3}\beta\alpha^3$, (5.80) can be satisfied if $\alpha$ is above a critical value $\alpha_c$,

$$\alpha_c \approx \left(\frac{3}{32\beta}\right)^{\frac{1}{3}} \quad , \tag{5.81}$$

provided that $\beta$ is sufficiently large; the corresponding critical density is $\propto \alpha_c^3 \propto \beta^{-1}$.

The above discussions, after some minor changes, can be extended to cases where $b^2 \neq 3ac$ and $m_N \neq g\,b/c$.

## 6. σ - Model

It is not our purpose here to start a complete re-investigation of the σ-model[11] of strong interactions; such a project clearly lies outside the scope of the present paper. However, as we shall see, there are some rather new and interesting properties in the σ-model when a sizable chunk of nuclear matter is present; these properties are closely related to those discussed above. In this section, we shall give only a brief survey of these new features. Our discussion will be restricted to the tree approximation.

The σ-model consists of a spin $\frac{1}{2}$ nucleon field $\psi$, a spin 0 (even parity) field $\sigma$ and the usual pseudoscalar pion field $\vec{\pi}$. The Lagrangian density is given, apart from the counter terms for renormalization, by

$$\mathcal{L} = -\psi^\dagger \gamma_4 \gamma_\mu \frac{\partial}{\partial x_\mu} \psi - g \psi^\dagger \gamma_4 \left[\sigma + i\vec{\pi}\cdot\vec{\tau}\gamma_5\right]\psi$$

$$-\tfrac{1}{2}\left[\left(\frac{\partial\sigma}{\partial x_\mu}\right)^2 + \left(\frac{\partial\vec{\pi}}{\partial x_\mu}\right)^2\right] - U_\sigma \quad , \tag{6.1}$$

where

$$U_\sigma = \tfrac{1}{4}\lambda^2\left[(\sigma^2+\vec{\pi}^2) - (\mu/\lambda)^2\right]^2 - C_\pi\sigma \quad . \tag{6.2}$$

For convenience, we assume the parameters $C_\pi$, $\mu$ and $\lambda$ to be all positive. The minimum of the c. number function $U_\sigma$ occurs at $\sigma = \sigma_0$ and $\vec{\pi} = 0$, where $\sigma_0$ is $> (\mu/\lambda)$ and satisfies

$$C_\pi = \sigma_0(\lambda^2\sigma_0^2 - \mu^2) \quad . \tag{6.3}$$

In the tree approximation, the renormalized constants $\lambda$, $\mu$, $g$ and $C_\pi$ are related to the physical masses $m_N$, $m_\sigma$ and $m_\pi$ of the particles by

$$m_N = g\sigma_0 , \qquad C_\pi = m_\pi^2 \sigma_0 ,$$

$$m_\pi^2 = \lambda^2 \sigma_0^2 - \mu^2 \tag{6.4}$$

and $$m_\sigma^2 = 3\lambda^2 \sigma_0^2 - \mu^2 .$$

The vacuum state satisfies

$$< \text{vac} \mid \sigma(x) \mid \text{vac} > = \sigma_0 \tag{6.5}$$

and $< \text{vac} \mid \vec{\pi}(x) \mid \text{vac} > = 0$. In the $\sigma$-model, the constant $g$ is given by the well-known $\pi$-nucleon coupling, $(4\pi)^{-1} g^2 \cong 15.7$. The only unknown parameter is $m_\sigma$. However from the absence of any $0+$ resonance that has been positively identified experimentally, we may conclude $m_\sigma$ is $\gg m_\pi$, and may perhaps be[12] $\sim O(m_N)$.

We note that if $\vec{\pi} = 0$, then $U_\sigma$ reduces to the form (1.2) with $\phi \propto (\sigma - \sigma_0)$. Owing to the smallness of $m_\pi$, and therefore also of $C_\pi$, the function $U_\sigma$ has a local maximum at $\sigma$ near zero and a local minimum, besides $\sigma = \sigma_0$, at $\sigma$ near $-\sigma_0$. However, when $\vec{\pi}$ is now allowed to vary, this local minimum at $\sigma$ near $-\sigma_0$ turns into a saddle point; it is connected to the absolute minimum point $\sigma = \sigma_0$ by a smooth path, $\sigma^2 + \vec{\pi}^2 \cong \sigma_0^2$, without passing through any potential barrier. Thus, in the absence of nuclear matter, the $\sigma$-model is quite different from the system discussed in the previous sections. On the other hand, when there is nuclear matter present in a certain

region, then for a sufficiently large nuclear density and the region not too small, the $\sigma$-model exhibits almost exactly the same property as that discussed in the previous sections.

It is convenient to introduce, similar to (5.9), the dimensionless variables:

$$\rho \equiv \sqrt{2}\,\mu r \qquad \text{and} \qquad X \equiv \lambda\sigma/\mu \tag{6.6}$$

[i.e., on account of (6.4), $\rho = (m_\sigma^2 - 3m_\pi^2)^{\frac{1}{2}} r$ and $X = (g\sigma/m_N)(m_\sigma^2 - m_\pi^2)^{\frac{1}{2}} \cdot (m_\sigma^2 - 3m_\pi^2)^{-\frac{1}{2}}$]. For simplicity, let us consider a spherical nucleus of radius $\rho = R$. Furthermore, just as in Sections 5.4 and 5.5, we assume for the nucleons a degenerate Fermi distribution with a maximum Fermi momentum $k_F$, given by (5.32). By following exactly the same discussion given in the previous two sections, we find that outside the nucleus the classical time-independent spherically symmetric equation for $\sigma$ (with $\vec{\pi} = 0$) is

$$\frac{1}{\rho^2}\,\frac{d}{d\rho}\left(\rho^2\,\frac{dX}{d\rho}\right) - \frac{d}{dX}V_\sigma(X) = 0 \tag{6.7}$$

where

$$V_\sigma(X) = \tfrac{1}{8}(1 - X^2)^2 - \eta X \tag{6.8}$$

and where because of (6.4), $\eta$ is given by

$$\eta = m_\pi^2 (m_\sigma^2 - m_\pi^2)^{\frac{1}{2}} (m_\sigma^2 - 3m_\pi^2)^{-\frac{3}{2}} \ll 1 \,. \tag{6.9}$$

Inside the nucleus, the corresponding equation is

$$\frac{1}{\rho^2}\frac{d}{d\rho}\left(\rho^2\frac{dX}{d\rho}\right) - \frac{d}{dX}V_\sigma(X) = j_N(X) \quad . \tag{6.10}$$

The function $j_N(X)$ depends on the nuclear model. Under the assumption of the "free gas model", we have $j_N = (j_N)_{gas}$ where, just as in (5.50),

$$(j_N)_{gas} = 2\beta X\left\{(\omega^2 - X^2)^{\frac{1}{2}}\omega - \tfrac{1}{2}X^2 \ln\left[\frac{\omega + (\omega^2 - X^2)^{\frac{1}{2}}}{X}\right]^2\right\}, \tag{6.11}$$

in which $\omega$ is a constant, related to the value of $X$ at $\rho = R$ by

$$X(R) = \omega \tag{6.12}$$

and, because of (6.4),

$$\beta = \frac{g^2 m_N^2}{2\pi^2(m_\sigma^2 - m_\pi^2)} \quad . \tag{6.13}$$

On the other hand, if we assume the "incompressible fluid model" then $j_N = (j_N)_{fluid}$ where, just as in (5.67) and (5.68),

$$(j_N)_{fluid} = 2\beta X\left\{\alpha(\alpha^2 + X^2)^{\frac{1}{2}} - \tfrac{1}{2}X^2 \ln\left[\frac{\alpha + (\alpha^2 + X^2)^{\frac{1}{2}}}{X}\right]^2\right\}, \tag{6.14}$$

in which $\beta$ is given by (6.13) and $\alpha$ is a constant related to the Fermi momentum $k_F$

by

$$\alpha = k_F / m_N \quad . \tag{6.15}$$

In the limit $m_\pi \to 0$, $\eta \to 0$ and the above equation (6.10) reduces identically to either (5.49) or (5.67).

In the $\sigma$-model, $(4\pi)^{-1} g^2 \cong 15.7$ and therefore (after neglecting $m_\pi^2$)

$$\beta \cong 10 (m_N/m_\sigma)^2 \quad . \tag{6.16}$$

In the free nucleon gas model, by using (5.61) we find

$$\omega \cong .44 (m_\sigma/m_N)^{1/2} \quad . \tag{6.17}$$

If we neglect the surface energy, then according to (5.62) the binding energy per nucleon is $(1-\omega) m_N$. Thus, in this model, if $m_\sigma$ is less than $\sim 5\, m_N$ there would be a new type of stable heavy nucleus, provided that the nucleon number is sufficiently large.

If we assume the incompressible fluid model, then the field energy is given by (5.70)-(5.72), except that $V(X)$ is now

$$V(X) = V_\sigma(X) + V_N(X) - V_N(1) \tag{6.18}$$

where $V_\sigma$ is given by (6.8), but $V_N$ remains given by (5.68). The above expression reduces to (5.73) in the limit $m_\pi = 0$. As noted in Section 5.5, when the nucleon density is sufficiently high, the minimum energy state of a very heavy nucleus flips from the

"normal" solution (in which $X$ is near 1 and the nucleon mass $\cong m_N$) to an "abnormal" one, in which both $X$ and the "effective" nucleon mass are near 0. In order to produce the flip to the "abnormal" solution, (5.80) must be satisfied. By using (5.81) and (6.16), one finds that the critical density is approximately determined by

$$a_c \equiv \left(\frac{k_F}{m_N}\right)_c \approx 0.21\left(\frac{m_\sigma}{m_N}\right)^{\frac{2}{3}} . \tag{6.19}$$

If $m_\sigma \cong m_N$, then the critical density is about the usual nuclear density

$$n_0 = \left[\frac{4\pi}{3}(1.3 \times 10^{-13}\ \text{cm.})^3\right]^{-1} . \tag{6.20}$$

If $m_\sigma \neq m_N$, then the critical density $n_c$ varies approximately as

$$n_c \approx n_0\left(\frac{m_\sigma}{m_N}\right)^2 , \tag{6.21}$$

provided that $m_\sigma$ is not too large.

In Figure 7, the function $V(X)$ is plotted for $m_\sigma = m_N$ and the usual nuclear density $n = n_0$, with $m_\pi \neq 0$. From the plot, one sees more explicitly that under these conditions, if the nucleus is sufficiently heavy (so that surface energy can be neglected) then, as expected, the "abnormal" solution has an energy comparable to that of the "normal" solution. If $m_\sigma$ is $> m_N$, one may produce the "abnormal" nuclear state by increasing the nuclear density through, say, high energy collisions between very heavy nuclei. From Figure 7, one observes that there is practically no

potential barrier between the "normal" and the "abnormal" configurations, once the critical density is reached; the corresponding production probability should, therefore, be relatively high.

## 7. Remarks

In this paper we have investigated, among other things, the possibility that over a limited region in space the expectation value $<\phi>$ of a spin 0 even parity field $\phi(x)$ may be different from its "normal" vacuum expectation value (which can be chosen, by convention, to be zero). This investigation leads us to a study of several different physical problems, each containing some rather interesting properties. However, not all of them have been fully examined in this paper.

If the spin 0 field has a strong interaction with some matter field, say the nucleon field with a large coupling $g$, then whenever there is a sizable bulk of nuclear matter present, there is a tendency to have $<\phi(x)> \cong -(m_N/g)$ in the region occupied by nuclear matter. This would reduce the "effective" nucleon mass to $\cong 0$, and thereby lower the kinetic energy of the nucleons. Within a certain range of the relevant physical parameters, this unusual solution may even become the lowest energy state. Thus, if such a strongly interacting scalar field does exist, there would be the possibility of a large class of "stable" or "metastable" superheavy nuclei, hitherto undiscovered.

As a mathematical model, such a possibility suggests also a possible extension to the boundstate description of a single nucleon, by replacing the role of nucleus by nucleon, and of nucleons by a mixture of "quarks" plus a suitable "quark-antiquark" continuum. Since the "effective" quark mass might be near zero inside the boundstate (though heavy outside), one could hope to resolve some of the present theoretical difficulties in such a description.

If the spin 0 field has a large $\phi^3$-coupling constant $b$, then the function $U(\phi)$, defined by (1.2), can have another local minimum at $\phi = \phi_{vex} \neq 0$. In this case, even without the presence of nuclear matter, there could be the possibility of a pure vacuum excitation state, in which the expectation value $<\phi(x)>$ is $\cong \phi_{vex}$ over an extended region in space. This leads naturally to the physical picture that the so-called "vacuum" actually more resembles a "medium" whose properties can be changed. If this is true, which of course we do not know at present, it must ultimately lead to rather striking physical consequences.

We wish to thank N. H. Christ, A. H. Mueller, L. M. Lederman and M. A. Ruderman for discussions.

## Appendix A

In this appendix we give the details of the graphical representation of the energy density function $\mathcal{E}(\bar{\phi})$, which is defined by (2.4). It is convenient to introduce the unrenormalized field operator $\phi_0$:

$$\phi_0 = Z^{\frac{1}{2}} \phi \tag{A.1}$$

where $\phi$ is the renormalized field operator, as before. The Lagrangian density (1.1) may be written as

$$\mathcal{L} = -\tfrac{1}{2}\left(\frac{\partial \phi_0}{\partial x_\mu}\right)^2 - \phi_0\,\delta J - \tfrac{1}{2}\phi_0^2(a + \delta a) - (3!)^{-1}\phi_0^3(b + \delta b) - (4!)^{-1}\phi_0^4(c + \delta c) \tag{A.2}$$

where $\delta J$, $\delta a$, $\delta b$ and $\delta c$ are counter terms; together with $(Z^{\frac{1}{2}} - 1)$, these terms are needed to cancel the infinities.

The counter term $\delta J$ is determined by requiring

$$\langle \text{vac} \mid \phi_0(x) \mid \text{vac} \rangle = 0 \quad . \tag{A.3}$$

The precise definitions of $\delta a$, $\delta b$ and $\delta c$ will be given below [after Eq. (A.23)].

From (2.1) and (2.2), the Hamiltonian $H_J$ may be written as the sum of a zeroth order term $H_0$ and a perturbation term $H_1$:

$$H_J = H_0 + H_1 \ , \tag{A.4}$$

$$H_0 = \tfrac{1}{2} \int \left[ \pi_0^2 + (\nabla \phi_0)^2 + a_0 \phi_0^2 \right] d^3r \quad , \tag{A.5}$$

$$H_1 = \int \left[ (J_0 + \delta J)\, \phi_0 + (3!)^{-1} b_0 \phi_0^3 + (4!)^{-1} c_0 \phi_0^4 \right] d^3r \quad , \tag{A.6}$$

where $\pi_0$ is the conjugate momentum of $\phi_0$,

$$a_0 = a + \delta a \quad , \qquad b_0 = b + \delta b \quad ,$$

$$c_0 = c + \delta c \quad , \tag{A.7}$$

and the constant $J_0$ is related to $J$, introduced in (2.1), by

$$J_0 = J Z^{-\frac{1}{2}} \quad . \tag{A.8}$$

Since the counter term $\delta J$ is determined by (A.3) in which $|\,\text{vac}\,\rangle$ is defined to be the lowest-energy eigenstate of $H_J$ with $J_0 = 0$, there should be a non-zero expectation value of $\phi(x)$ in the lowest-energy eigenstate $|\,\rangle$ of $H_J$ when $J_0 \neq 0$. We define

$$\bar{\phi}_0 = \Omega^{-1} \int \langle\, | \phi_0(x) | \,\rangle \, d^3r \quad . \tag{A.9}$$

Both $\bar{\phi}_0$ and the corresponding lowest eigenvalue $\lambda_J$ of $\Omega^{-1} H_J$ may be evaluated by regarding $H_0$ as the unperturbed Hamiltonian and $H_1$ as the perturbation. The perturbation series of $\lambda_J$ is the sum of all connected Feynman graphs that have no external line. We may write

$$\lambda_J = (\lambda_J)_{\text{tree}} + (\lambda_J)_{\text{one-loop}} + (\lambda_J)_{\text{two-loop}} + \cdots \tag{A.10}$$

in which $(\lambda_J)_{\text{tree}}$ denotes the partial summation of all such diagrams that are trees and $(\lambda_J)_{\ell\text{-loop}}$ denotes the partial summation of all such diagrams that have $\ell$ loops.

From (A.6), (A.9) and (2.3), one sees that keeping $a_0$, $b_0$ and $c_0$ fixed

$$\frac{\partial \lambda_J}{\partial J_0} = \bar{\phi}_0 \quad . \tag{A.11}$$

We recall that according to (2.4)

$$\mathcal{E}(\bar{\phi}_0) = \lambda_J - J_0 \bar{\phi}_0 \quad . \tag{A.12}$$

Thus, keeping $a_0$, $b_0$ and $c_0$ fixed, we have

$$\frac{\partial \mathcal{E}}{\partial \bar{\phi}_0} = - J_0 \tag{A.13}$$

and

$$(\partial^2 \mathcal{E}/\partial \bar{\phi}_0^2)\,(\partial^2 \lambda_J/\partial J_0^2) = -1 \quad . \tag{A.14}$$

Tree Diagrams

In Figure 8, we list the sum $(\lambda_J)_{\text{tree}}$ of all the tree diagrams. In these diagrams, there is no external line. Every internal line carries a zero 4-momentum, so it gives to the Feynman amplitude a factor $-i\,(k^2 + a_0)^{-1}$ with $k = 0$. Every one-point vertex gives a factor $-i\,J_0$, every three-point vertex a factor $-i\,b_0$ and every four-point vertex a factor $-i\,c_0$. From Figure 8, it follows that, keeping $a_0$, $b_0$

and $c_0$ fixed, (A. 11) holds within the tree approximation; i.e., $(\partial \lambda_J / \partial J_0)_{tree} = \bar{\phi}_0$. Furthermore, in the same tree approximation, the full propagator of $\phi_0$ at the zero 4-momentum is simply $i(\partial^2 \lambda_J / \partial J_0^2)_{tree}$. Thus, one derives

$$(\partial^2 \lambda_J / \partial J_0^2)_{tree} = -(k^2 + a_0 + b_0 \bar{\phi}_0 + \tfrac{1}{2} c_0 \bar{\phi}_0^2)^{-1}_{k=0} \quad . \qquad \text{(A. 15)}$$

Because of (A. 14), this leads to

$$(\partial^2 \mathcal{E} / \partial \bar{\phi}_0^2)_{tree} = a_0 + b_0 \bar{\phi}_0 + \tfrac{1}{2} c_0 \bar{\phi}_0^2 \quad . \qquad \text{(A. 16)}$$

Again from Figure 8, one sees that as $J_0 \to 0$, $(\lambda_J)_{tree} \to 0$ and $(\partial \lambda_J / \partial J_0)_{tree} \to 0$. Therefore, as $\bar{\phi}_0 \to 0$, one must have $(\mathcal{E})_{tree} \to 0$ and $(\partial \mathcal{E} / \partial \bar{\phi}_0)_{tree} \to 0$. Consequently,

$$\left[\mathcal{E}(\bar{\phi}_0)\right]_{tree} = \tfrac{1}{2} a_0 \bar{\phi}_0^2 + (3!)^{-1} b_0 \bar{\phi}_0^3 + (4!)^{-1} c_0 \bar{\phi}_0^4 \quad . \qquad \text{(A. 17)}$$

General Expression

To find the general expression of $\mathcal{E}(\bar{\phi}_0)$, let us consider the scattering of n zero-momentum mesons whose interaction is given by the Lagrangian density (A. 2), and n may vary from 2 to $\infty$. We define $\left[S(\bar{\phi}_0)\right]_{loop}$ to be the sum of all such one-particle irreducible scattering diagrams that are not trees; in these diagrams, each external line carries a zero 4-momentum and gives a factor $\bar{\phi}_0$ to the Feynman integral. The corresponding factors for the internal line, the three-point vertex and the four-point vertex are, respectively, $-i(k^2 + a_0)^{-1}$, $-i b_0$ and $-i c_0$. [Note that there is

no one-point vertex in these scattering graphs. ] We shall now establish

$$\mathcal{E}(\bar{\Phi}_0) = \left[\mathcal{E}(\bar{\Phi}_0)\right]_{tree} + \left[iS(\bar{\Phi}_0)\right]_{loop} . \qquad (A.18)$$

To prove this, we consider the sum (A. 10) and note that, similarly to (A. 15)

$$i\frac{\partial^2 \lambda_J}{\partial J_0^2} = \left[\mathcal{D}_J(k)\right]_{k=0} \qquad (A.19)$$

where $\mathcal{D}_J(k)$ is the full propagator of the meson field $\phi_0$ in a theory in which the Hamiltonian is given by (A.4). We may write

$$\left[i\mathcal{D}_J(k)\right]^{-1} = k^2 + a_0 + i\Sigma(k) \qquad (A.20)$$

where $\Sigma(k)$ is, by definition, the sum of all proper self-energy diagrams. Let us separate in $\Sigma(k)$ the $J_0$-dependent part $\Sigma_J(k)$ from the $J_0$-independent part $\Sigma_0(k)$ :

$$\Sigma(k) = \Sigma_0(k) + \Sigma_J(k) \qquad (A.21)$$

where as $J_0 \to 0$, $\Sigma_J(k) \to 0$ and therefore $\Sigma(k) \to \Sigma_0(k)$. According to (A.6), the dependence on $J_0$ is completely due to the one-point vertex. Thus, every diagram in $\Sigma_J(k)$ is one-particle reducible. I.e., it is possible to separate every diagram in $\Sigma_J(k)$ into two disconnected parts by cutting an internal line open; one of these two disconnected parts contains the external momentum $k_\mu$, and the other does not. By repeating this cutting procedure and keeping only the part that contains $k_\mu$, each of

these diagrams can be reduced to a one-particle irreducible diagram in which there is no $J_0$-vertex, but besides the two external lines that carry $k_\mu$, we have also other zero-momentum external lines (as the remainder of the cutting). If we assign to each of these additional zero-momentum external lines a factor $\bar{\phi}_0$ to the Feynman amplitude, we find $\Sigma_J(k)$, introduced in (A.21), is equal to the summation over the set of all such different one-particle irreducible (proper self-energy) diagrams. In this set, for $k \neq 0$ every diagram has at least one zero-momentum external line. Among these diagrams, there are only two diagrams without any loop; these are simply $-ib_0\bar{\phi}_0$ and $-i\frac{1}{2}c_0\bar{\phi}_0^2$. The rest all have some loops.

Next, we note that for $k \neq 0$ the $J_0$-independent part $\Sigma_0(k)$, defined in (A.20), consists of all one-particle irreducible proper self-energy diagrams that do not have any zero-momentum external line. Together, $\Sigma(k) = \Sigma_0(k) + \Sigma_J(k)$ is then the sum of all one-particle irreducible proper self-energy diagrams which may or may not have additional zero-momentum external lines. It is now straightforward to show that $\left[S(\bar{\phi}_0)\right]_{\text{loop}}$, defined above, is related to $\Sigma(k)$ at $k = 0$ by

$$i\Sigma(0) = b_0\bar{\phi}_0 + \tfrac{1}{2}c_0\bar{\phi}_0^2 + \frac{\partial^2}{\partial\bar{\phi}_0^2}\left[iS(\bar{\phi}_0)\right]_{\text{loop}} . \qquad \text{(A.22)}$$

By using (A.14) and the boundary condition that at $\bar{\phi}_0 = 0$, both $\mathcal{E}$ and $(\partial\mathcal{E}/\partial\bar{\phi}_0)$ vanish. We establish (A.18).

Equations (A.17) and (A.18) still differ from (3.1) and (3.2) by being expressed in terms of $a_0$, $b_0$, $c_0$ and $\bar{\phi}_0$ rather than the corresponding renormalized quantities. We note that whatever may be the precise definitions of these renormalized quantities,

formally the counter terms $\delta a$, $\delta b$, $\delta c$ and $(Z^{\frac{1}{2}} - 1)$ can always be expressed as sums over the appropriate set of diagrams in which only the renormalized quantities $a$, $b$, $c$ and $\bar{\phi}$ appear. Every one of these diagrams must have loops. By redefining "loop" to include also these loops in the counter term, we derive (3.1) and (3.2).

Renormalized Constants

To define the wave function renormalization constant $Z$, we may follow the standard procedure: Set $J_0 = 0$. The full propagator of the $\phi_0$ field becomes then

$$\mathcal{D}_0(k) = -i\left[k^2 + a_0 + \Sigma_0(k)\right]^{-1} \tag{A.23}$$

where $\Sigma_0(k)$ is defined in (A.21). Let $k^2 = -m_\phi^2$ be the zero of $\left[\mathcal{D}_0(k)\right]^{-1}$. We require as $k^2 \to -m_\phi^2$

$$\left[\mathcal{D}_0(k)\right]^{-1} \to iZ^{-1}(k^2 + m_\phi^2) \quad . \tag{A.24}$$

Thus, $Z$ is defined, and $m_\phi$ is the physical mass of the meson. The renormalized constant $a$ is defined by

$$\mathcal{D}_0(k) \to \frac{-iZ}{a} \qquad \text{as} \qquad k^2 \to 0 \quad . \tag{A.25}$$

Consequently,

$$a = \left[a_0 + \Sigma_0(0)\right] Z \quad . \tag{A.26}$$

From (A.18), (A.22) and the fact that $\Sigma(k) \to \Sigma_0(k)$ as $\bar{\phi} \to 0$, we obtain in the same

limit $\bar{\phi} \to 0$,

$$\mathcal{E}(\bar{\phi}) \to \tfrac{1}{2} a \bar{\phi}^2 + O(\bar{\phi}^3) \quad . \tag{A.27}$$

We may expand the scattering amplitude $\left[S(\bar{\phi}_0)\right]_{\text{loop}}$ as a power series in $\bar{\phi}_0$ :

$$\left[S(\bar{\phi}_0)\right]_{\text{loop}} = \sum_{n=2}^{\infty} (n!)^{-1} S_n \bar{\phi}_0^{\,n} \tag{A.28}$$

in which n denotes the number of external mesons in the scattering amplitude. From (A.21), (A.22) and (A.26), it follows that

$$a = \left[a_0 + i S_2\right] Z \quad . \tag{A.29}$$

Since $S_2$ contains a quadratically divergent Feynman integral, two counter terms $\delta a$ and $(Z - 1)$ are needed to render (A.29) finite. The renormalized coupling constants b and c are related to the scattering amplitudes $S_3$ and $S_4$ by

$$b + \text{finite term} = \left[b_0 + i S_3\right] Z^{\frac{3}{2}} \tag{A.30}$$

and

$$c + \text{finite term} = \left[c_0 + i S_4\right] Z^2 \quad . \tag{A.31}$$

Since $S_3$ and Z both contain only logarithmically divergent integrals, one counter term $\delta b$ is sufficient to render (A.30) finite; similarly, one counter term $\delta c$ is sufficient to render (A.31) finite. The precise values of the finite terms in (A.30) and (A.31) are determined by imposing (3.8), as discussed in Section 3.2.

If one wishes, one may alter the above definition of $Z$ by an arbitrary finite multiplicative factor, say $Z \to \zeta Z$, provided that $a \to \zeta a$, $b \to \zeta^{\frac{3}{2}} b$, $c \to \zeta^2 c$ and $\bar{\phi} \to \zeta^{-\frac{1}{2}} \bar{\phi}$; of course, the residue of the renormalized propagator at $k^2 + m_\phi^2 = 0$ now becomes not 1 but $\zeta^{-1}$.

## Appendix B

According to the rules for the prototype diagram, given in Section 3.1, the Feynman amplitude for diagram (i) in Figure 2 is given by

$$(i) \;=\; \tfrac{1}{2}(-ic)\, I^2 \tag{B.1}$$

where the factor $\frac{1}{2}$ denotes the inverse of the symmetry number, and

$$I = \frac{-i}{(2\pi)^4} \int \frac{d^4k}{k^2 + a(1+\Delta)} - \text{constant} - \text{constant} \cdot \Delta \tag{B.2}$$

in which the two constants are determined by requiring $I$ to be $O(\Delta^2)$ as $\Delta \to 0$. The integral (B.2) can be readily evaluated. We find

$$I = (16\pi^2)^{-1}\, a\left[(1+\Delta)\ln(1+\Delta) - \Delta\right] . \tag{B.3}$$

According to (A.18), in order to obtain $\mathcal{L}(\bar{\phi})$, we should multiply the scattering amplitude (B.1) by $i$; this gives the first term on the righthand side of (3.17).

The evaluation of the prototype diagram (ii) in Figure 2 is complicated since it can be made finite only after we include also the diagram (ii)'. According to the rules given in Section 3.1, we find

$$(ii) \;=\; \frac{-ib^2}{(3!)(2\pi)^8} \int \frac{d^4k\, d^4q}{\left[k^2 + a(1+\Delta)\right]\left[q^2 + a(1+\Delta)\right]\left[(k+q)^2 + a(1+\Delta)\right]}$$

$$+ \text{subtraction} \;, \tag{B.4}$$

$$(ii)' = \frac{-\delta a}{(2\pi)^4} \int \frac{d^4k}{k^2 + a(1+\Delta)} + \text{subtraction} , \qquad (B.5)$$

and, to the lowest order,

$$\delta a = \frac{-ib^2}{2(2\pi)^4} \int \frac{d^4q}{(q^2+a)^2} \qquad (B.6)$$

where, according to (3.8), the subtraction terms must be quadratic functions of $\Delta$. Since both integrals in (B.4) and (B.5) are not primitively divergent, even with the subtraction terms included, (ii) and (ii)' are still logarithmically divergent. It is convenient to introduce another diagram, diagram (v) in Figure 2, in which the dashed line denotes the propagator $-i(k^2+a)^{-1}$. [The solid line remains $-i(k^2+a+a\Delta)^{-1}$.]

$$(v) = \frac{-ib^2}{2(2\pi)^8} \int \frac{d^4k\, d^4q}{(k^2+a)(q^2+a)\left[(k+q)^2+a(1+\Delta)\right]}$$

$$+ \text{subtraction} . \qquad (B.7)$$

Again, the subtraction term is assumed to be a quadratic function in $\Delta$. We shall calculate first (ii)' + (v) and (ii) - (v) separately, and then sum these two terms together. By using the standard parametric representation of the Feynman integral, one can show that

$$(ii)' + (v) = \frac{iab^2}{2(16\pi^2)^2} \int \prod_1^3 dx_j\, \delta\Big(\sum_1^3 x_j - 1\Big)\, F(x_2\, \Delta)$$

$$\times \left[(x_1x_2 + x_2x_3 + x_1x_3)^{-2} - x_2^{-2}(x_1+x_3)^{-2}\right] \qquad (B.8)$$

where $x_j \geq 0$ and the function $F$ is

$$F(y) = (1+y)\ln(1+y) - y - \tfrac{1}{2}y^2 \quad . \tag{B.9}$$

Similarly, we find

$$(ii) - (v) = \frac{iab^2}{3!(16\pi^2)^2} \int \prod_1^3 dx_j \, \delta\Big(\sum_1^3 x_j - 1\Big)(x_1x_2 + x_2x_3 + x_1x_3)^{-2}$$

$$\times \Big[F(\Delta) - \sum_{j=1}^{3} F(x_j\Delta)\Big] \quad . \tag{B.10}$$

Both expressions are now finite. It is straightforward to verify that

$$(ii) + (ii)' = \frac{iab^2}{2(16\pi^2)^2}\Big[F(\Delta) - G(\Delta)\Big] \tag{B.11}$$

where

$$G(\Delta) = \tfrac{1}{2}(1+\Delta)\Big[\ln(1+\Delta)\Big]^2 - (1+\Delta)\ln(1+\Delta) + \Delta \quad . \tag{B.12}$$

By using Theorem 1, one sees that diagrams (iii) + (iii)' and (iv) + (iv)' are related to (ii) + (ii)' in a simple way. Their entire sum is given by (B. 11), provided one substitutes $b^2$ by $b^2 + 2ac\Delta$, but keeping $a$ and $\Delta$ fixed. Equation (3. 17) is then established, and this completes the proof of Theorem 2.

## Appendix C

To establish Theorem 3 (stated in Section 3.3), we shall consider first the case $\ell > 3$ and $c = 0$. One can readily verify that in this case, there is no primitively divergent prototype diagram; consequently, we need only consider the convergent ones. A typical example is given by diagram (i) in Figure 9. Let $I$ and $V$ be, respectively, the number of internal lines and vertices in the diagram. We have

$$2I = 3V \quad , \qquad \ell = I - V + 1 \quad ,$$

and therefore

$$V = 2(\ell - 1) \quad . \tag{C.1}$$

Since each vertex carries a factor $b$, the corresponding Feynman amplitude is proportional to $b^V$. The dimension of the energy density function is $(\text{mass})^4$. Thus, from a simple dimensional consideration and by using (C.1), one sees that the amplitude should be proportional to $a^2 (b^2/a)^{\ell-1}$. Now, according to the rules for the prototype diagram given in Section 3.1, the parameter $a$ appears only in the product $a(1 + \Delta)$; this implies that the amplitude is proportional to

$$a^2 (b^2/a)^{\ell-1} (1 + \Delta)^{\ell-3} \quad . \tag{C.2}$$

Since the diagram is a convergent one, one finds the proportionality constant to be finite and independent of $\Delta$. Equation (3.19) now follows because of (3.8).

Next, we consider the case $\ell = 3$ and $c = 0$. In this case, there is only one primitively divergent prototype diagram, given by (ii) in Figure 9. By writing down explicitly the corresponding Feynman amplitude, one can readily derive (3.18). Theorem 3 is then proven.

## Appendix D

In this appendix, we give an estimate of a lower bound for the decay rate $\lambda_L$, defined in (4.6). Let us expand the field operator $\phi(\vec{r}, t)$ in terms of the Fourier series in the volume $L^3$:

$$\phi(\vec{r}, t) = q_0 + \sum_{\vec{k}\neq 0} q_k e^{i\vec{k}\cdot\vec{r}} \quad . \tag{D.1}$$

The Lagrangian for the system inside $L^3$ is

$$\int \mathcal{L}\, d^3r = \tfrac{1}{2} L^3 \left[\left(\frac{dq_0}{dt}\right)^2 - U(q_0)\right] + \cdots \tag{D.2}$$

where $U$ is given by (1.2), and $\cdots$ is $q_k$-dependent $(\vec{k} \neq 0)$. The conjugate momentum of $q_0$ is

$$p_0 = L^3 \left(\frac{dq_0}{dt}\right) \quad . \tag{D.3}$$

Therefore, the Hamiltonian is

$$H = \tfrac{1}{2}\left[L^{-3} p_0^2 + L^3 U(q_0)\right] + \cdots \quad . \tag{D.4}$$

According to (4.1), at time $t = 0$ the system is at $q_0 = \phi_{vex}$ which is only a local minimum of $U(q_0)$. There is a potential barrier that separates this local minimum from the absolute minimum of $U(q_0)$, which is at $q_0 = 0$. To estimate the barrier-penetration probability, we shall use the W. K. B. method for the $q_0$ degree

of freedom, but suppress all other $\vec{k} \neq 0$ degrees of freedom (i.e., set $q_k = 0$ for $\vec{k} \neq 0$). The result is

$$\lambda_L \sim \omega \exp \left[ - 2L^3 \int \left[ U(q_0) - U(\phi_{vex}) \right]^{\frac{1}{2}} dq_0 \right] \qquad (D.5)$$

where

$$\omega^2 = a + b\phi_{vex} + \tfrac{1}{2} c \phi_{vex}^2 \quad . \qquad (D.6)$$

In (D.5), the integration is from $q_0 = \phi_{vex}$ to $q_0'$ where $U(q_0') = U(\phi_{vex})$ and $\phi_{vex} < q_0' \leq 0$. Such an estimation of $\lambda_L$ is obviously an underestimation, since by using the other $\vec{k} \neq 0$ degrees of freedom, one can easily show that there are other paths leading from the local minimum $q_0 = \phi_{vex}$ to regions near the absolute minimum $q_0 = 0$, but passing through a much lower potential barrier.

References


1. For a history of this subject, see Y. Nambu in Fields and Quanta 1, 33 (1970)
2. J. Goldstone, Nuovo Cimento 19, 155 (1961).

   J. Goldstone, A. Salam and S. Weinberg, Phys. Rev. 127, 965 (1962).

   P. W. Higgs, Phys. Letters 12, 132 (1964); Phys. Rev. Letters 13, 508 (1964); Phys. Rev. 145, 1156 (1966), and literature cited there and in Ref. 1.
3. T. D. Lee and C. N. Yang, Phys. Rev. 87, 404, 417 (1952)
4. S. Coleman and E. Weinberg, Phys. Rev. D7, 1888 (1973)
5. See, e.g., T. D. Lee and C. N. Yang, Phys. Rev. 117, 22 (1960)
6. See, e.g., K. Symanzik, Comm. Math. Phys. 16, 48 (1970). Calculations very similar to those given here may be found in B. W. Lee, Nucl. Phys. B9, 649 (1969).
7. Notions essentially identical to the "prototype diagram" have been used in many-body problems and statistical mechanics. See Ref. 5.
8. F. J. Dyson, Phys. Rev. 75, 1736 (1949)
9. See, e.g., R. Finkelstein, R. Le Levier and M. Ruderman, Phys. Rev. 83, 326 (1951)
10. One may wonder, as $\phi$ varies from 0 to a non-zero value, what happens to the energy change of the Dirac sea of negative energy states. Naively, one might expect the increment $\Delta\mathcal{E}$ in energy density to be given by the difference

$$d \equiv \Omega^{-1}\left\{\Sigma\left[p^2+m_N^2\right]^{\frac{1}{2}} - \Sigma\left[p^2+(m_N+g\phi)^2\right]^{\frac{1}{2}}\right\}$$

   where $\Omega$ is the volume of the system. Since the summation extends over all negative energy states, the expression for $d$ is $\infty$ if $\phi \neq 0$. Actually,

$\Delta\mathcal{E} \neq d$. By following the argument given in Section 3, one can show that $\Delta\mathcal{E}$ should be given by the appropriate sum of all nucleon loop diagrams. If we include only the one-nucleon-loop approximation, then $\Delta\mathcal{E}$ is equal to the above expression $d$, but only after a subtraction of a fourth-order polynomial in $\phi$; its explicit expression, after summing over both proton and neutron, is

$$\Delta\mathcal{E} = -\frac{1}{8\pi^2}\left\{(m_N+g\phi)^4 \ln\left[(m_N+g\phi)^2/m_N^2\right] - 2g\phi\left[m_N^3 + \frac{7}{2}m_N^2 g\phi + \frac{13}{3}m_N(g\phi)^2 + \frac{25}{12}(g\phi)^3\right]\right\} .$$

At $m_N + g\phi = 0$, $\Delta\mathcal{E} = (16\pi^2)^{-1} m_N^4$. In a complete treatment, one should, of course, include $\Delta\mathcal{E}$ in $U_\phi(-m_N/g)$, together with other corrections due to higher order Fermion as well as all Boson loops. [Note that $6\pi^2\,\Delta\mathcal{E} = \frac{3}{8}m_N^4 < m_N^4$, therefore the inequality (5.45) is not violated.] In this section, our discussion is, however, restricted to the semi-classical equation, without taking into account any loop correction.

11. J. Schwinger, Ann. Phys. 2, 407 (1957).
J. C. Polkinghorne, Nuovo Cimento 8, 179, 781 (1958).
M. Gell-Mann and M. Lévy, Nuovo Cimento 16, 53 (1960).
For further references, see those given in B. W. Lee, Chiral Dynamics (Gordon and Breach, 1972).

12. For the present experimental status, e.g., see the review article by Protopopesen et al. in the Proceedings of the Philadelphia Conference on Experimental Meson Spectroscopy—1972, ed. A. H. Rosenfeld and K. W. Lai (American Institute of Physics).

## Figure Captions

Figure 1. Examples of graphs of $\mathcal{E}(\bar{\phi})$ and $J(\bar{\phi}) = -(d\mathcal{E}/d\bar{\phi})$ in the tree approximation. The two-phase region is between the points $\alpha$ and $\beta$; $\phi_\alpha$ and $\phi_\beta$ are their abscissae. In the top graph, outside the interval $\phi_\alpha \leqq \bar{\phi} \leqq \phi_\beta$, $\mathcal{E}(\bar{\phi}) = U(\bar{\phi})$; inside the interval, the solid line refers to $\mathcal{E}$, and the dashed curve to $U$. In the bottom graph, the two areas $C\,\alpha\,A$ and $C\,\beta\,B$ (between the dashed curve and the solid line) are equal.

Figure 2. Diagrams (i)—(iv) are examples of two-loop prototype diagrams. Each solid internal line carries a propagator factor $D$, given by (3.3). Diagrams (ii)'—(iv)' are related to (ii)—(iv) through renormalization. In diagram (v), the dashed line carries a factor $-i(k^2 + a)^{-1}$; hence (v) is not a prototype diagram.

Figure 3. $J$ in unit $\frac{ab}{c}$ vs. $\bar{\phi}$ in unit $\frac{b}{c}$ for the special case $b^2 = 3ac$ and $(32\pi^2)^{-1} c = 10^{-1}$. The solid curve denotes the tree approximation, and the dashed curve includes the one-loop approximation.

Figure 4. Phase-space diagram for the mechanical analogy discussed in Section 5.2. Inside the region $\mathcal{R}$, the minimal $K$ is $-\frac{1}{8}$ at the origin. The dashed curve illustrates a spiral solution.

Figure 5. $X$ vs. $\frac{dX}{d\rho}$ at $\rho = R$. The "outside" curves refer to solutions of (5.48); integrating from $\rho = \infty$ to $R$. The "inside" curves refer to solutions of (5.49), integrating from $\rho = 0$ to $R$, with $\beta = 10$.

Figure 6. Numerical solution of $X(\rho)$ in the free nucleon gas model. The total number of nucleons is $\cong 210$ and the top Fermi energy is $\omega\, m_N \cong 0.46\, m_N$. The nuclear radius is $R = 20$, and the nucleon density $n$ is zero outside the nucleus, but $\propto (\omega^2 - X^2)^{\frac{3}{2}}$ inside.

Figure 7. $V(X)$ in the $\sigma$-model for a nucleon density $n = \left[\frac{4\pi}{3}(1.3 \times 10^{-13}\,\text{cm})^3\right]^{-1}$ and for $n = 0$. See Eq. (6.18) for the definition of $V(X)$.

Figure 8. Tree diagrams for $\lambda_J$ and its derivatives. All lines carry zero 4-momentum. For the Feynman amplitude, there is a factor $-(i/a_0)$ to each line, $-i J_0$ to each one-point vertex, $-i b_0$ to each three-point vertex and $-i c_0$ to each four-point vertex. Each open circle denotes a differentiation with respect to $(-i J_0)$.

Figure 9. Examples of prototype diagrams in a $\phi^3$-theory. Diagram (i) is convergent, and diagram (ii) is primitively divergent.

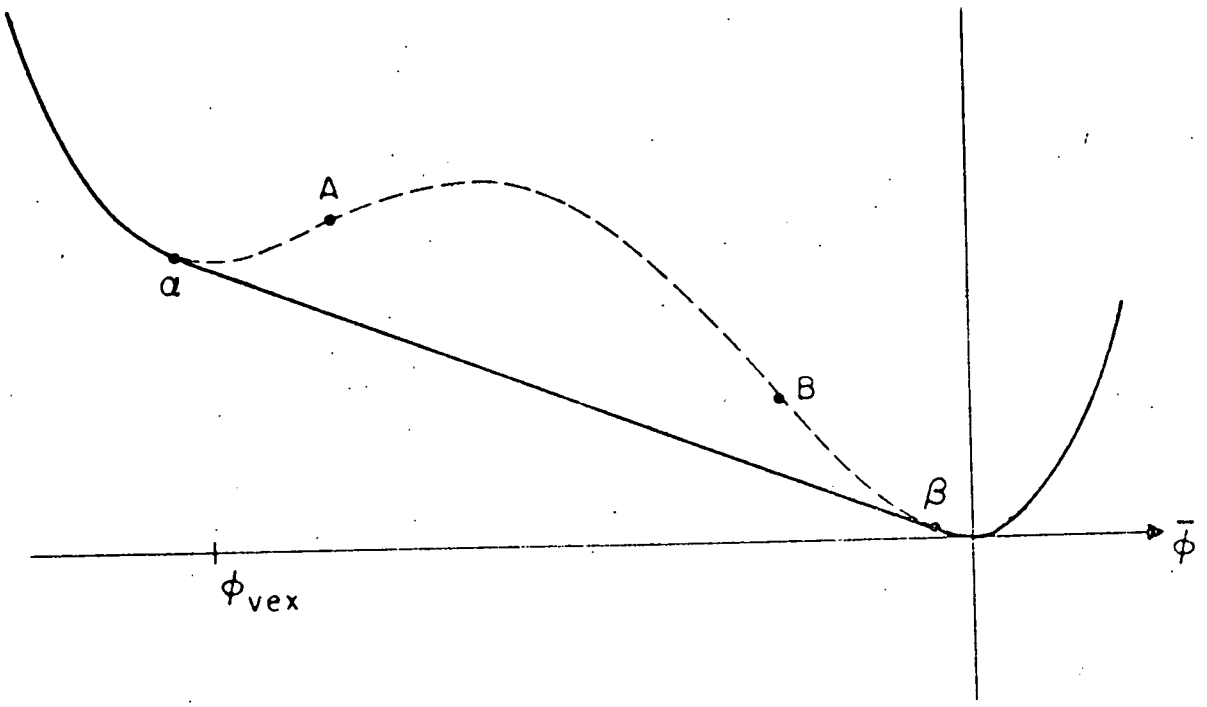


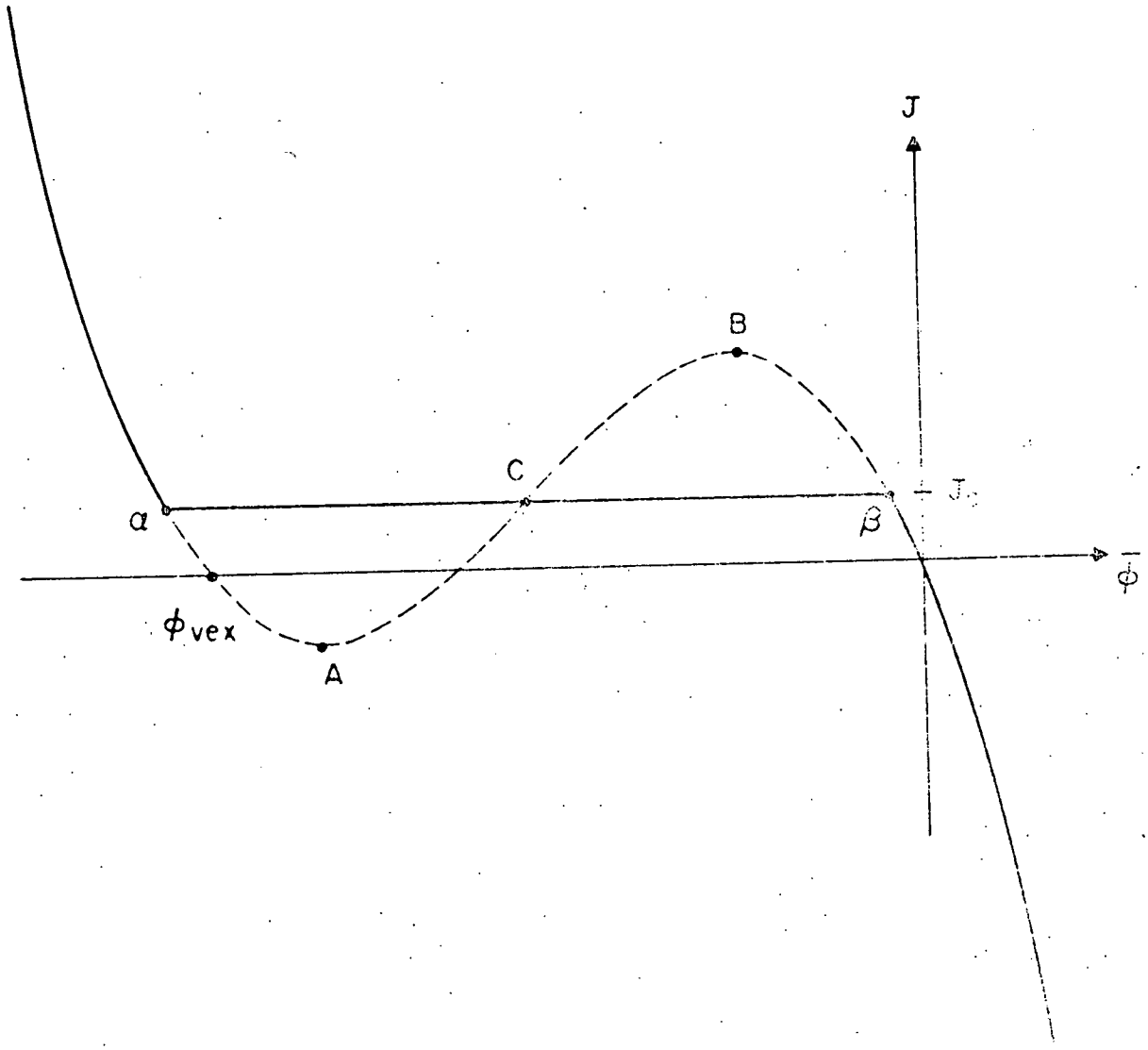


Fig. 1

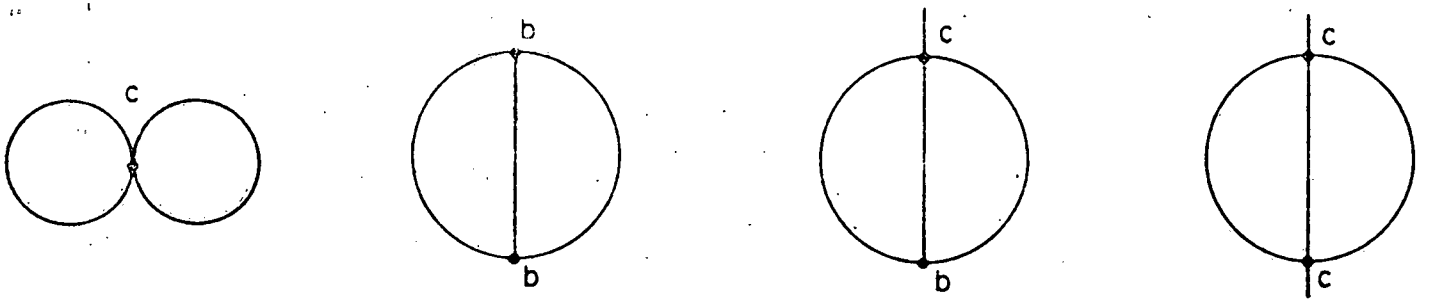


(i) (ii) (iii) (iv)

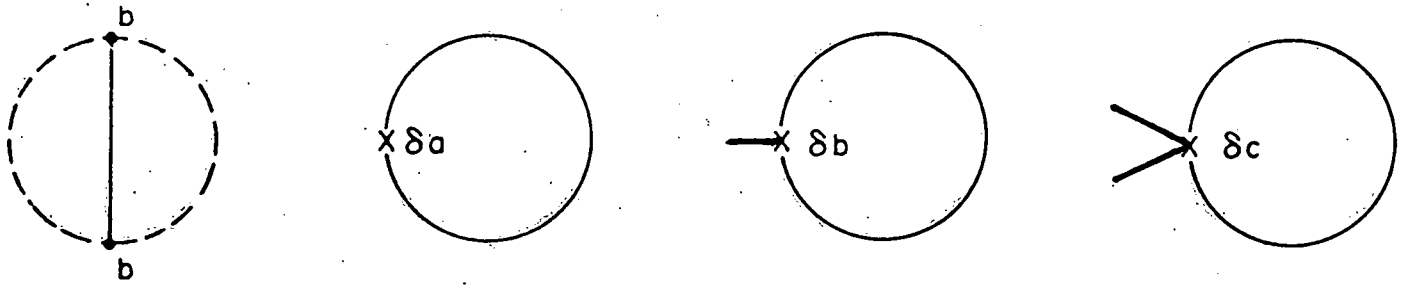


(v) (ii)′ (iii)′ (iv)′

Fig. 2

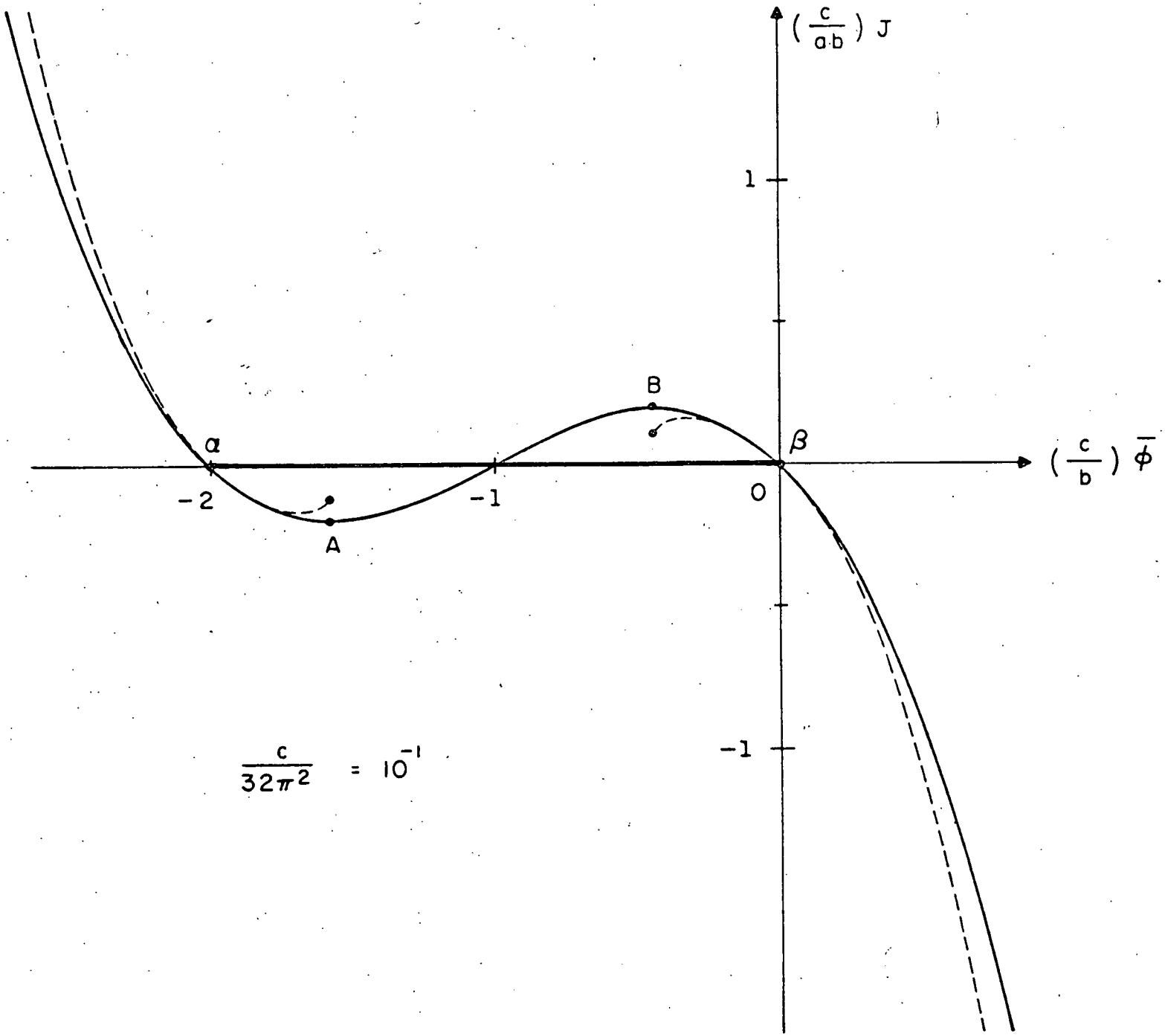


Fig. 3

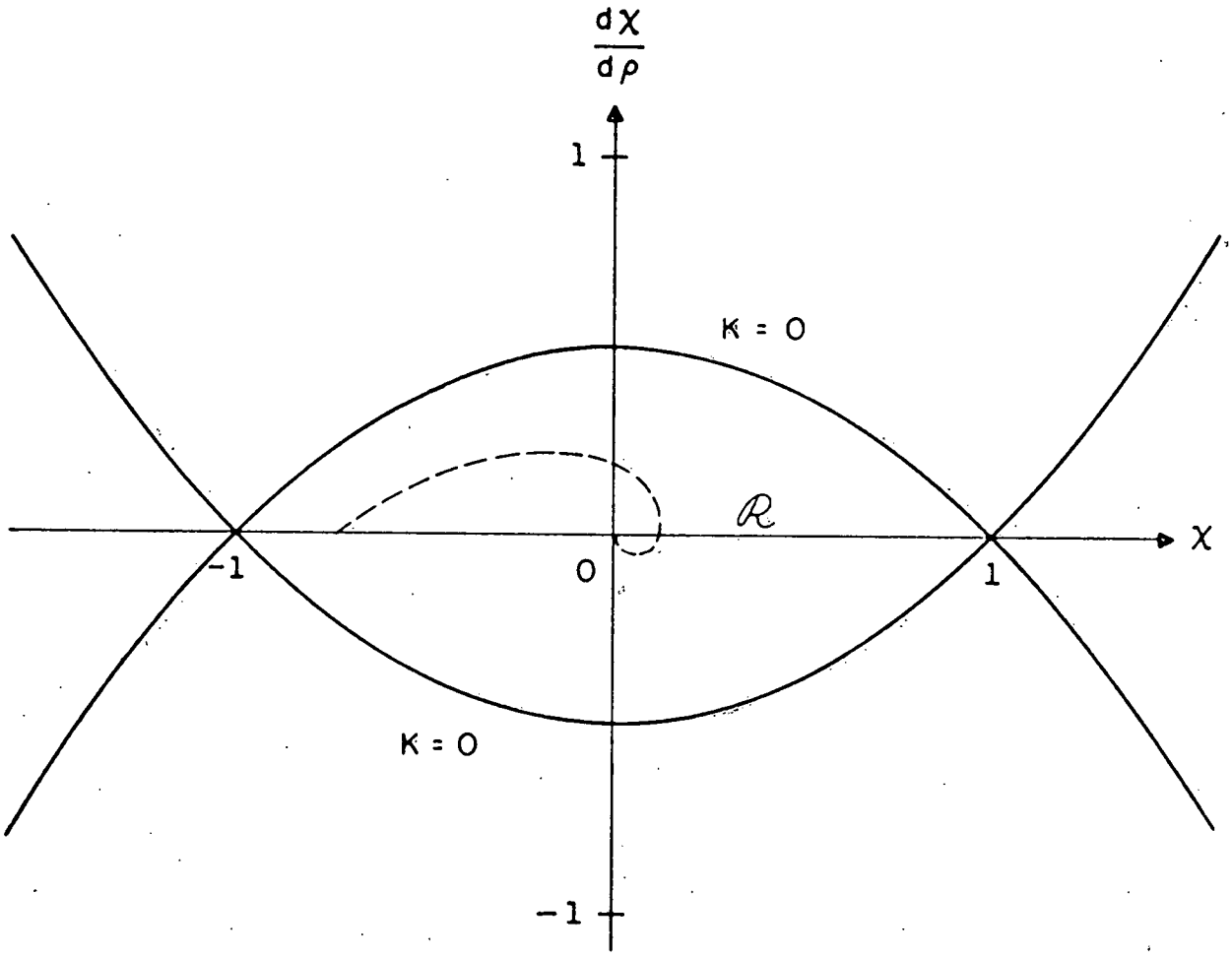


Fig. 4

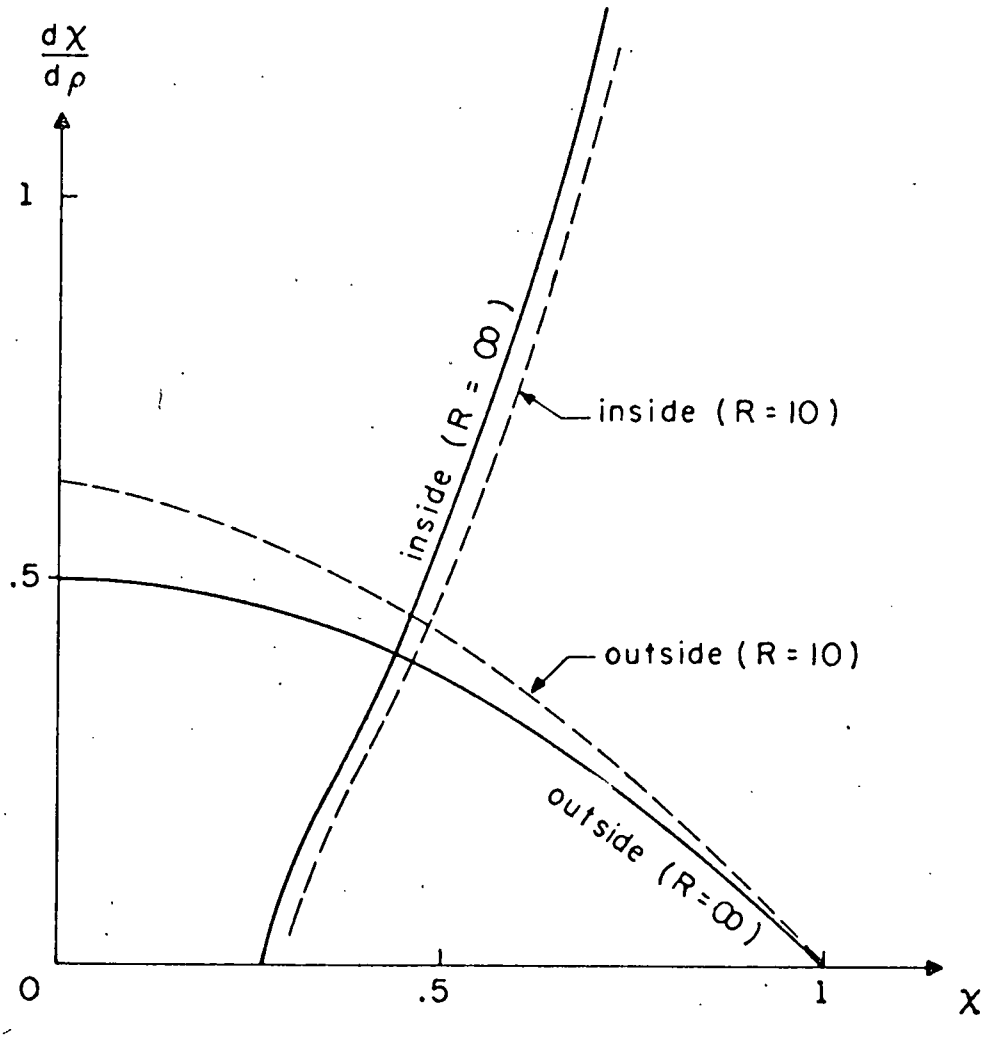


Fig. 5

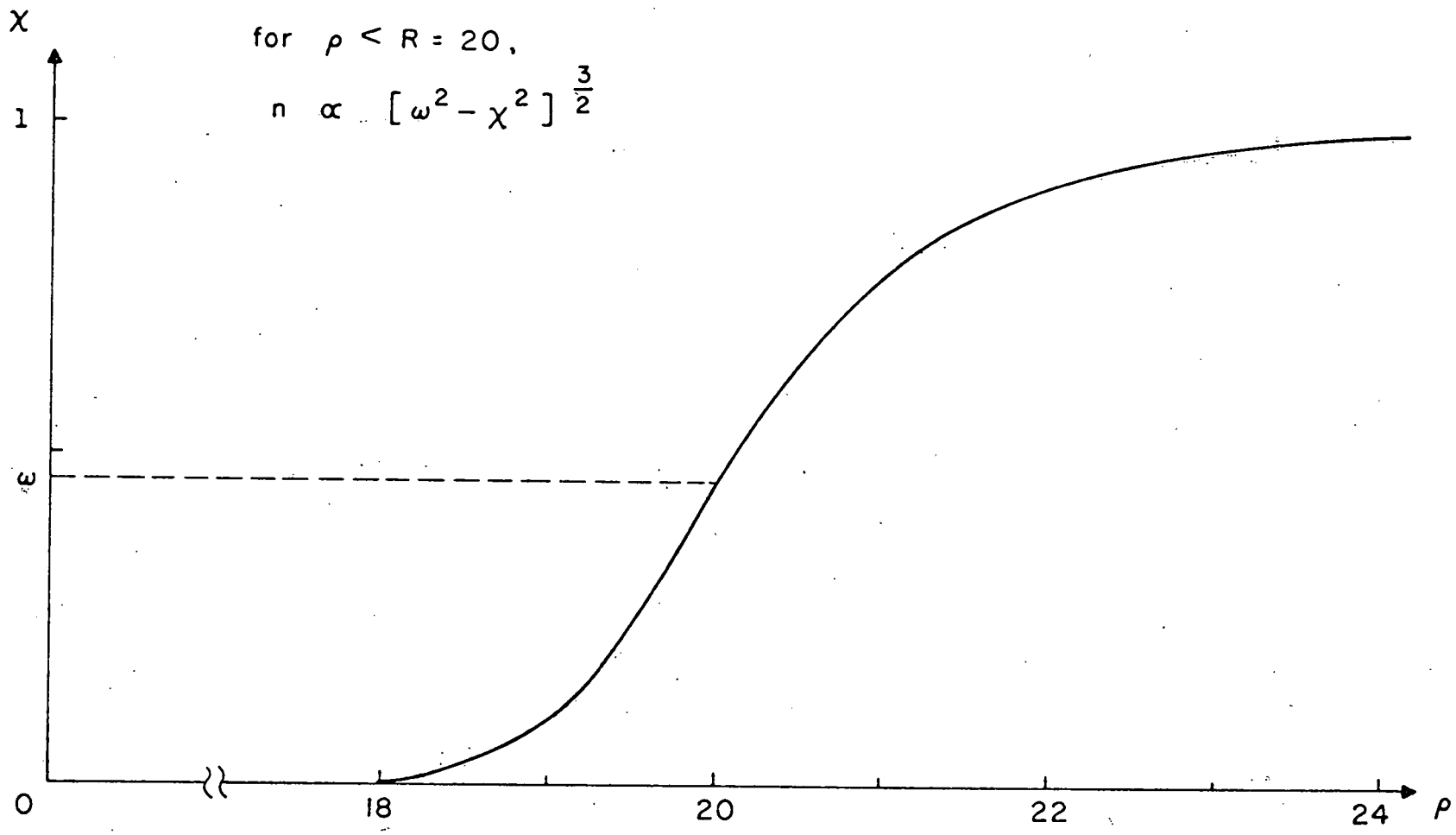


Fig. 6

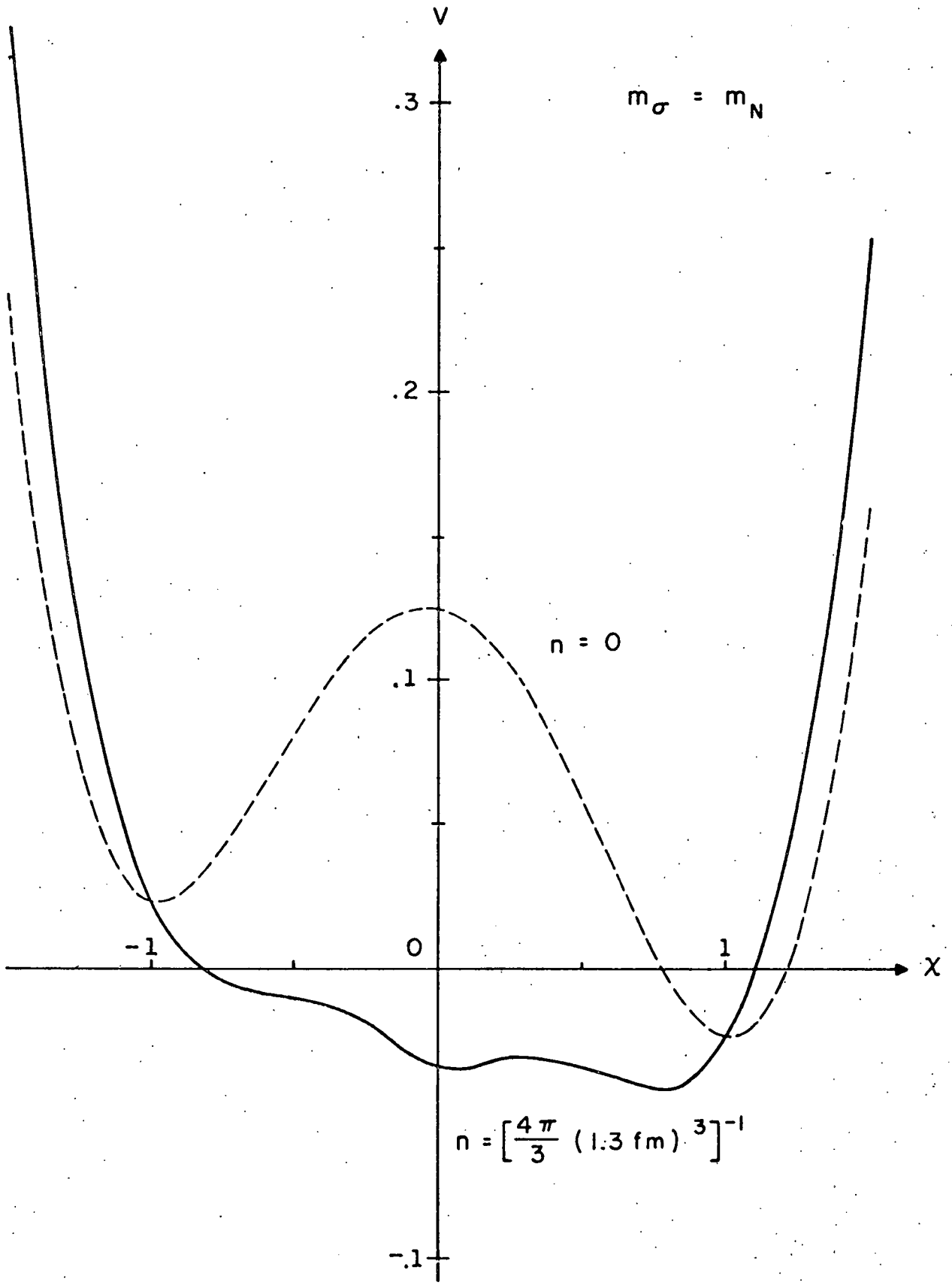


Fig. 7

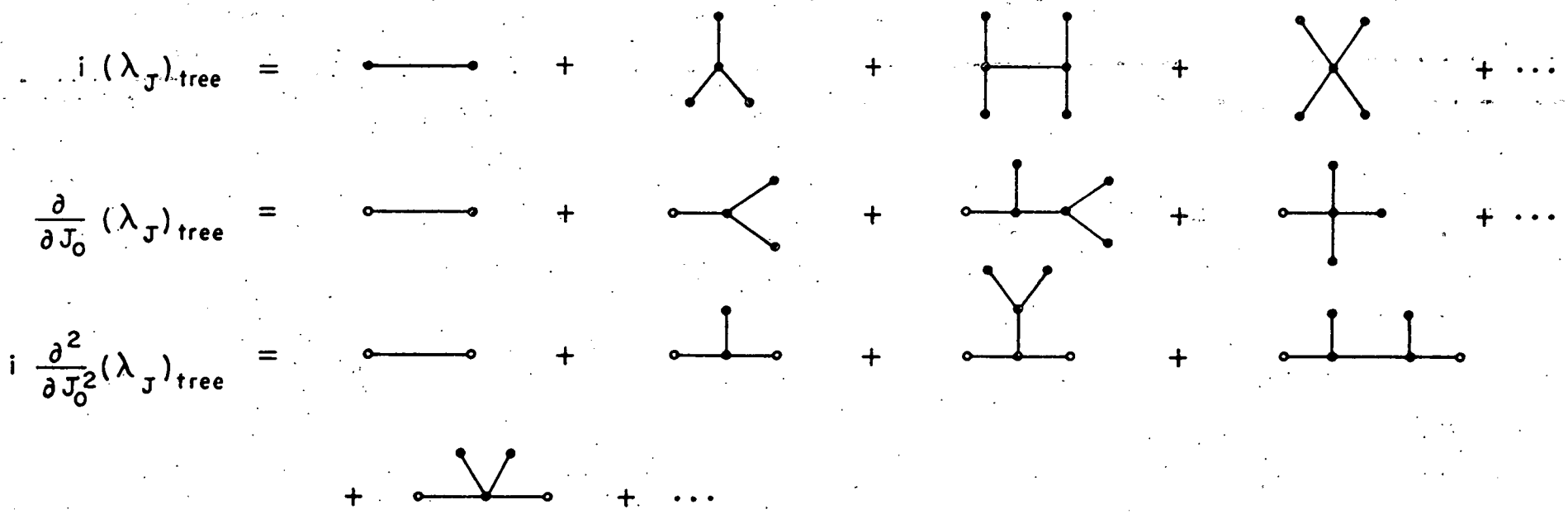
$i\,(\lambda_J)_{tree}$ =
+
+
+
+ ...
$\frac{\partial}{\partial J_0}\,(\lambda_J)_{tree}$ =
+
+
+
+ ...
$i\,\frac{\partial^2}{\partial J_0^2}(\lambda_J)_{tree}$ =
+
+
+
+ ...

Fig. 8

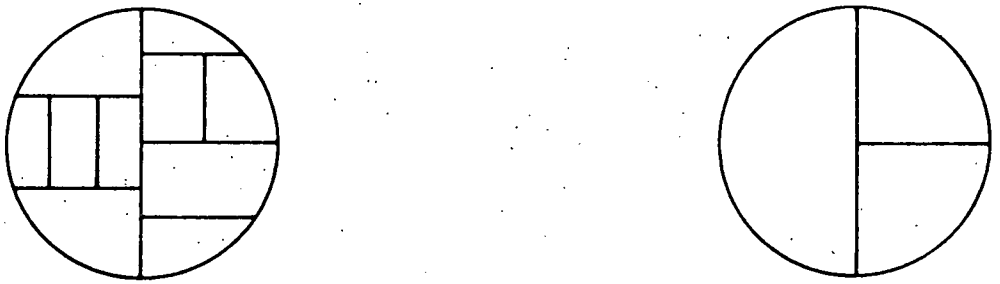
(i)
(ii)

Fig. 9